

**Charm as a domain wall fermion in quenched lattice QCD**Huey-Wen Lin,<sup>1,\*</sup> Shigemi Ohta,<sup>2,3,4,†</sup> Amarjit Soni,<sup>5,‡</sup> and Norikazu Yamada<sup>2,3,§</sup><sup>1</sup>*Physics Department, Columbia University, New York, New York 10027, USA*<sup>2</sup>*Institute of Particle and Nuclear Studies, KEK, Ibaraki 305-0801, Japan*<sup>3</sup>*The Graduate University for Advanced Studies (Sokendai), Tsukuba, Ibaraki 305-0801, Japan*<sup>4</sup>*RIKEN BNL Research Center, Brookhaven National Laboratory, Upton, New York 11973, USA*<sup>5</sup>*Department of Physics, Brookhaven National Laboratory, Upton, New York 11973, USA*

(Received 21 August 2006; published 13 December 2006)

We report a study describing the charm quark by a domain-wall fermion (DWF) in lattice quantum chromodynamics (QCD). Our study uses a quenched gauge ensemble with the DBW2 rectangle-improved gauge action at a lattice cutoff of  $a^{-1} \sim 3$  GeV. We calculate masses of heavy-light (charmed) and heavy-heavy (charmonium) mesons with spin-parity  $J^P = 0^\mp$  and  $1^\mp$ , leptonic decay constants of the charmed pseudoscalar mesons ( $D$  and  $D_s$ ), and the  $D^0$ - $\bar{D}^0$  mixing parameter. The charm quark mass is found to be  $m_c^{\overline{\text{MS}}}(m_c) = 1.24(1)_{\text{stat}}(18)_{\text{sys}}$  GeV. The mass splittings in charmed-meson parity partners  $\Delta_{q,J=0}$  and  $\Delta_{q,J=1}$  are degenerate within statistical errors, in accordance with experiment, and they satisfy a relation  $\Delta_{q=ud,J} > \Delta_{q=s,J}$ , also consistent with experiment. Using our lattice calculation of the splitting between  $h_c$  and  $\chi_{c1}$  and the experimental  $\chi_{c1}$  mass, we obtain a parity-odd axial-vector charmonium state  $m_{h_c} = 3533(11)_{\text{stat}}(336)_{\text{sys}}$  MeV, with a systematic error dominated by heavy quark discretization at order  $(am_c)^2$ . However, in this regard, we emphasize significant discrepancies in the calculation of hyperfine splittings on the lattice. The leptonic decay constants of  $D$  and  $D_s$  mesons are found to be  $f_D = 232(7)_{\text{stat}}({}^{+6}_{-0})_{\text{chiral}}(17)_{\text{sys}}$  MeV and  $f_{D_s}/f_D = 1.05(2)_{\text{stat}}({}^{+0}_{-2})_{\text{chiral}}(2)_{\text{sys}}$ , where the first error is statistical, the second is systematic due to chiral extrapolation, and the third error is a combination of other known systematics. The  $D^0$ - $\bar{D}^0$  mixing bag parameter, which enters the  $\Delta C = 2$  transition amplitude, is found to be  $B_D(2 \text{ GeV}) = 0.845(24)_{\text{stat}}({}^{+24}_{-6})_{\text{chiral}}(105)_{\text{sys}}$ . All the above systematic errors include our estimates of quenching errors.

DOI: [10.1103/PhysRevD.74.114506](https://doi.org/10.1103/PhysRevD.74.114506)

PACS numbers: 11.15.Ha, 12.38.Gc, 13.20.Fc, 14.40.Lb

**I. INTRODUCTION**

Properties of hadrons containing one or more charm quarks have been intensively investigated in recent experiments [1–10]. While the main purpose of these experiments is to acquire information useful or necessary to the phenomenology of the Cabibbo-Kobayashi Maskawa (CKM) quark mixing matrix, it is also exciting that several new hadron states have been discovered and confirmed in these experiments. For the latest reviews on these new states, see, for example, Refs. [11–13]. Lattice QCD should be able to describe various features of these new states. However, in lattice calculations of heavy quark systems, the discretization error associated with masses as large as the lattice cutoff makes the interpretation of numerical results ambiguous. One possible way to avoid this systematic error is to rely on an effective theory such as heavy quark effective theory (HQET) [14–16] or nonrelativistic QCD (NRQCD) [17,18]. With such an approach, however, one must discard either the ability to study quarkonia or to take the continuum limit. An alternative is to rely on a relativistic method with brute numerical force. Thanks to rapid growth of computational resources, discretization errors in this approach for a heavy quark which

is relatively light (like the charm) are beginning to be brought under control. Several studies have already been made in this direction [19–23].

In this work, we explore the feasibility of applying the domain-wall fermion (DWF) [24–26] as a heavy quark within the quenched approximation. Domain-wall fermions have been successfully applied to calculations of the light hadron spectrum and weak matrix elements [27–31]. The primary advantage of working with this fermion action is its ability to retain continuumlike chiral symmetry even at a finite lattice spacing, by adding a fifth dimension to the lattice. The size of the symmetry breaking is represented by the residual mass,  $am_{\text{res}}$ , which is adjusted by changing the fifth-dimensional extent of the lattice and is of the order of  $10^{-3}$  in lattice units in state-of-the-art calculations. It is known that the presence of exact chiral symmetry guarantees the absence of  $O(a)$  discretization errors, and, in the domain-wall case, the violation of the order of  $am_{\text{res}}$  implies that the leading error is significantly suppressed. Thus it seems to be a natural extension to apply the DWF formalism to heavier,  $c$  and  $b$ , quarks. To make the next-to-leading-order discretization error [ $\sim O((am_q)^2)$ ] as small as possible, our calculations are carried out on relatively fine lattices with  $a^{-1} \sim 3$  GeV. Although this study is done in the quenched approximation, the experience should be useful in future studies with dynamical fermions.

One way to test a given heavy quark formalism is to see how consistently the formalism describes both heavy-

\*Electronic address: [hwlin@theory1.phys.columbia.edu](mailto:hwlin@theory1.phys.columbia.edu)†Electronic address: [shigemi.ohta@kek.jp](mailto:shigemi.ohta@kek.jp)‡Electronic address: [soni@bnl.gov](mailto:soni@bnl.gov)§Electronic address: [norikazu.yamada@kek.jp](mailto:norikazu.yamada@kek.jp)

heavy and heavy-light systems with a single value of the mass parameter. While a single mass parameter does not have to describe both systems completely consistently in the quenched approximation and at a finite lattice spacing, making a quantitative test at some point will offer a reference for future work. Although we do not take a continuum limit here, such a study should become easier in the near future as available computational resources grow.

Once the charm quark mass is determined, it is interesting to see how well the lattice calculation reproduces the mass spectrum of recently discovered hadrons: the excited  $D$  meson states with spin-parity  $J^P = 0^+$  and  $1^+$ . The spectrum of these mesons had been studied before their discoveries by two groups based on chiral quark models [32,33]. These turned out to describe some qualitative features well. After the experimental discoveries, these groups refined their analyses quantitatively [34,35]. The studies suggest that chiral symmetry in the light quark sector plays an important role in the spectrum of these mesons. Since we apply the domain-wall formalism to both heavy and light quarks, we expect to get better descriptions of these mesons than earlier works with Wilson-type light quarks.

We would also like to make a lattice study of flavor physics, especially weak matrix elements of  $D$  mesons. As an example, we present the  $D$  meson leptonic decay constants and the bag parameter,  $B_D$ , relevant to  $D^0-\bar{D}^0$  mixing. Experiments are currently searching for evidence of mixing in the neutral  $D$ -meson system [5]. Since the expected amplitude is very small in the standard model, once it has been discovered, it would provide an important probe of physics beyond the standard model (see, e.g., Ref. [36]). Unlike the neutral  $B$  meson system, in  $D^0-\bar{D}^0$  mixing it is not clear whether the short-distance contribution mediated by a local four-quark operator dominates over long-distance contributions. Even so, it is still sensible to have an idea about the size of the short-distance contribution. Knowing the size of  $B_D$  will also be useful when evaluating  $B_B$  by extrapolation in quark mass. In this paper we present the first DWF charm lattice study of this quantity. Note that there were Wilson fermion studies earlier such as Refs. [37,38].

The first exploratory study of massive DWF was done in Refs. [39,40], which looked into the low-lying eigenmodes of the five-dimensional Hermitian domain-wall Dirac operator in detail and their dependence on the bare quark mass,  $am_q$ . All eigenmodes are classified into one of two kinds of states. The first are the physical, or “decaying,” states which are bound to the four-dimensional domain walls located at either end of the fifth dimension. Their wave functions fall exponentially away from the wall. When  $am_q \ll 1$ , these states dominate the low-lying eigenmodes of the whole system and describe four-dimensional physics. The other class contains unphysical, or “propagating,” states, which have nonzero momentum

in the fifth dimension. Their eigenvalues are large,  $\sim O(1/a)$ . From the viewpoint of the four-dimensional effective theory, these states are unphysical, a source of nonlocality that can invalidate the effective theory. The gap between these two types of states is controlled by the domain-wall height “ $M_5$ ” parameter. In the study of Refs. [39,40], it turned out that as  $am_q$  increases the absolute values of the eigenvalues of the decaying states rapidly increase, and the binding to the domain walls becomes less tight or even unbound. On the other hand, the eigenvalues of the propagating states increase only slowly. Thus, if  $am_q$  further increases, at some point the lowest eigenmode in the system will be one of the propagating states. Then one might worry that something wrong happens to the four-dimensional effective theory. In the past quenched studies [39,40], this mass threshold can be as low as 0.2 (in lattice units) for both  $\beta = 6.0$  Wilson gauge action and  $\beta = 0.87$  DBW2 gauge action, and 0.4 for  $\beta = 1.04$  DBW2 gauge action with  $M_5 = 1.8$ . In the present work, as will be described, a higher lattice coupling is used for the DBW2 gauge action. This results in a threshold of  $am_q \sim 0.5$  or higher in lattice units, while the bare charm quark mass is below 0.4.

The rest of the paper is organized as follows. In Sec. II we summarize our numerical methods and their parameters. Then meson mass spectra and charm mass analyses are presented in Sec. III. Section IV presents results for decay constants. We will also present the first DWF calculation of the mixing parameter,  $B_D$ , in Sec. V. The  $SU(3)$ -breaking ratio is discussed in Sec. VI. Extrapolations in  $1/m_{\text{heavy}}$  to the static limit are reported in Sec. VII. Some systematic errors are discussed in Sec. VIII. Section IX concludes with a summary and future outlook for this program. Preliminary results on spectrum and decay constants in this work are reported in Refs. [41–43].

## II. NUMERICAL METHOD AND PARAMETERS

The numerical lattice QCD calculations reported in this paper were performed in the quenched approximation using the QCDSF computers at RIKEN-BNL Research Center and Columbia University. The gauge configurations were generated in a previous RBC work determining the neutral kaon mixing bag parameter,  $B_K$  [44], with the DBW2 rectangle-improved gauge action [45,46] with gauge coupling  $\beta = 1.22$ . With the 106 gauge configuration in total used in that study, the lattice cutoff measured from the  $\rho$  meson mass is  $a_\rho^{-1} = 2.914(54)$  GeV. This implies a physical spatial volume for the  $24^3 \times 48$  lattices of about  $(1.6 \text{ fm})^3$ . We will use this cutoff estimate as a standard in this report. If we use the static quark potential instead, we obtain  $a_{r_0}^{-1} = 3.09(2)$  GeV [44]. Notice that the difference between these two determinations is about 5%, which is smaller than found on coarser lattices.

TABLE I. Ensemble parameters.

Quantities	Numbers
# of conf.	103
$a^{-1}$	2.914(54) GeV
$L_s$	10
$M_5$	1.65
$am_{\text{res}}$	$0.9722(27) \times 10^{-4}$
$am_{\text{light}}$	0.008, 0.016, 0.024, 0.032, 0.040
$am_{\text{heavy}}$	0.1, 0.2, 0.3, 0.4, 0.5

Of the 106 gauge configurations reported in the earlier study, in the present work we use only 103, due to the shutdown of the QCDSF computers in early 2006. This results in slight differences in the estimations of observables. We confirmed they are not significant.

We use DWF [24–26] to describe both heavy (charm) and light (up, down, strange) quarks. The number of sites in the fifth dimension,  $L_s = 10$ , and the domain-wall height,  $M_5 = 1.65$ , are taken to be the same as in the previous work [44]. The simulation parameters and some numerical results obtained in Ref. [44] which are relevant to this work are summarized in Table I. As seen from the table, our choice of parameters results in a residual mass of  $O(10^{-4})$  in lattice units, about 0.3 MeV. To study the quark mass

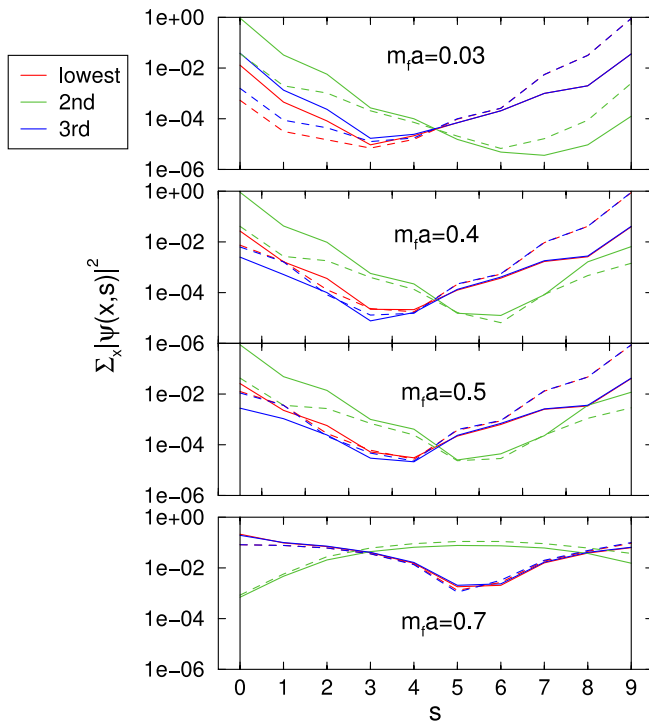


FIG. 1 (color online). Fifth-dimensional  $s$  dependence of the three eigenvectors of  $D_H$  with the smallest eigenvalues [both right-projection (dashed line) and left-projection (solid line) are displayed]:  $|\Psi_s^2|$  (with the  $y$  axis in log scale) with  $m_f \in \{0.03, 0.4, 0.5, 0.7\}$ . The propagating states only arise for  $am_f > 0.5$ .

TABLE II. Meson states in this study are created by local operators of the form  $\bar{\psi}\Gamma\psi$  in this table. Their spin and parity are also listed, as well as charge conjugation for quarkonium cases.

$\Gamma$	$2S+1L_J$	$J^{PC}$
$\gamma_5$	$^1S_0$	$0^{-+}$
$\gamma_i$	$^3S_1$	$1^{--}$
1	$^3P_0$	$0^{++}$
$\gamma_5\gamma_i$	$^3P_1$	$1^{++}$
$\gamma_i\gamma_j$		$1^{+-}$

dependence in a comprehensive way, we use five values each for heavy and light quark masses as listed in Table I. They, respectively, cover approximate ranges of  $[\frac{1}{4}m_{\text{charm}}, \frac{5}{4}m_{\text{charm}}]$  and  $[\frac{1}{4}m_{\text{strange}}, \frac{5}{4}m_{\text{strange}}]$ . Note that our choice of the heavy mass appears reasonable: Fig. 1 shows the eigenfunctions  $|\Psi_s^2|$  in the fifth dimension for the lowest three eigenvalues with various masses: 0.03, 0.4, 0.5, 0.7. The largest mass in the present work for the heavy quark is 0.5, and, as shown in the plot, its lowest three eigenstates drop exponentially away from the walls and so do not appear to be unphysical.

Table II lists the meson operators,  $\bar{\psi}\Gamma\psi$ , used in this work. We used source/sink combinations of wall-wall (denoted as  $C_{\text{ww}}^{\Gamma_1\Gamma_2}$ ) and wall-point (denoted as  $C_{\text{wp}}^{\Gamma_1\Gamma_2}$ ) types for two- and three-point functions. The source position is set at  $t_{\text{src}} = 7$ . The gauge fields are fixed to Coulomb gauge. The quark propagators are obtained by solving under periodic and antiperiodic boundary conditions in time and averaging over them. This procedure effectively doubles the period in time. In the calculations of two-point functions, we double the statistics by using an additional set of correlators with  $t_{\text{src}} = 41$ .

As was mentioned in the Introduction, we calculate the masses of heavy-light ( $D$  and  $D_s$ ) and heavy-heavy (charmonium) mesons with spin-parity  $J^P = 0^\mp$  and  $1^\mp$ , decay constants of the pseudoscalar mesons, and the  $D^0$ - $\bar{D}^0$  mixing parameter. We use the standard single-elimination jackknife method for statistical error analysis. Further details of numerical methods used in calculating respective quantities are summarized at the beginning of the sections reporting the results.

### III. SPECTROSCOPY

The meson masses are extracted by fitting the wall-point two-point correlators to the hyperbolic form

$$\mathcal{A} \cosh(m(t - L_t)), \quad (1)$$

after shifting the wall source time slice of the correlators to  $t = 0$ .

Using the 103 configurations, we first repeated the measurement of light meson spectroscopy as in Ref. [44], and confirmed that the differences from that reported in

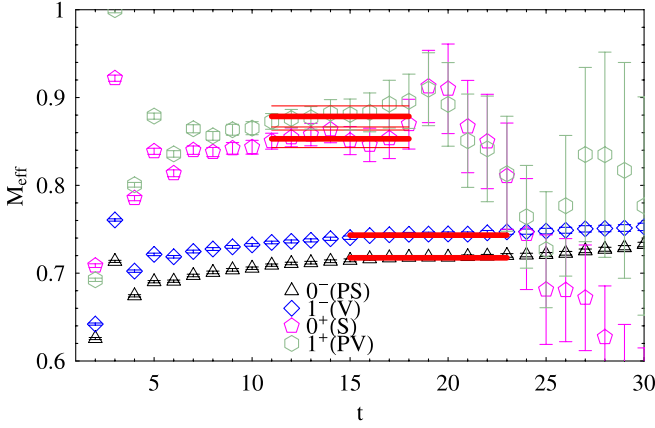


FIG. 2 (color online). Effective mass plots with the combination closest to the bare charm and strange mass simulation points:  $am_{\text{heavy}} = 0.4$  and  $am_{\text{light}} = 0.032$ .

Ref. [44] using full 106 configurations are negligible. For example and for later use, we present the bare strange quark mass in lattice units here. We choose to use  $m_K$  and  $m_\rho$  as inputs to determine the strange quark mass. The light quark pseudoscalar masses are fit to the form  $m_{\text{PS}}^2 = c_0 + c_1(m_q + m_{\text{res}})$ , while the light vector meson masses

are fit linearly as  $m_V = b_0 + b_1(m_q + m_{\text{res}})$ . Using the same fit ranges and the same functional forms in chiral extrapolation as in Ref. [44], we obtain  $am_{\text{strange}} = 0.0298(13)$ , which is consistent with  $am_{\text{strange}} = 0.0295(14)$  quoted in Ref. [44].

### A. Charmed mesons

The effective mass plots for the heavy-light mesons with the four different spin-parity states we are discussing are shown in Fig. 2 for  $am_{\text{heavy}} = 0.4$  and  $am_{\text{light}} = 0.032$ , which are the closest combination to the bare charm (obtained below) and strange (discussed above) mass, respectively. As seen from the figure, the plots for all four mesons show reasonable plateaux with this mass combination. Similar qualities of plateaux are obtained for the other combinations of  $am_{\text{heavy}} = 0.2, 0.3, 0.4,$  and  $0.5$  and  $am_{\text{light}} = 0.024, 0.032,$  and  $0.040$  as well. In addition, for the pseudoscalar ( $0^-$ ) and vector ( $1^-$ ) channels, we could also extract the masses for the mass combinations of  $am_{\text{heavy}} = 0.1$  and  $am_{\text{light}} = 0.008$  and  $0.016$ . We take the fit ranges as  $15 \leq t \leq 23$  for  $0^-$  and  $1^-$  states, and  $10 \leq t \leq 16$  for  $0^+$  and  $1^+$ . The numerical results for meson masses are summarized in Tables III, IV, V, and VI.

TABLE III. Heavy-light  $J^P = 0^-$  meson mass obtained from fitting to the hyperbolic cosine form in the range of  $15 \leq t \leq 23$ .

$m_{\text{heavy}}$	$m_{\text{light}}$	$m_{\text{PS}}$	$\chi^2$ per d.o.f.
0.1	0.008	0.3254(15)	0.22
	0.016	0.3373(13)	0.15
	0.024	0.3495(12)	0.09
	0.032	0.3617(11)	0.08
	0.040	0.3739(11)	0.07
0.2	0.008	0.4715(17)	0.36
	0.016	0.4812(14)	0.30
	0.024	0.4913(13)	0.23
	0.032	0.5016(12)	0.19
	0.040	0.5120(11)	0.18
0.3	0.008	0.5916(19)	0.51
	0.016	0.6003(15)	0.46
	0.024	0.6095(13)	0.37
	0.032	0.6189(12)	0.32
	0.040	0.6285(11)	0.31
0.4	0.008	0.6917(21)	0.71
	0.016	0.7000(16)	0.70
	0.024	0.7086(14)	0.59
	0.032	0.7175(13)	0.52
	0.040	0.7266(12)	0.49
0.5	0.008	0.7734(22)	0.84
	0.016	0.7815(17)	0.92
	0.024	0.7898(15)	0.84
	0.032	0.7984(14)	0.78
	0.040	0.8072(13)	0.75

TABLE IV. Heavy-light  $J^P = 1^-$  meson mass obtained from fitting to the hyperbolic cosine form in the range of  $15 \leq t \leq 23$ .

$m_{\text{heavy}}$	$m_{\text{light}}$	$m_{\text{PS}}$	$\chi^2$ per d.o.f.
0.1	0.008	0.4083(45)	0.55
	0.016	0.4153(35)	0.40
	0.024	0.4223(30)	0.27
	0.032	0.4310(26)	0.20
	0.040	0.4401(24)	0.17
0.2	0.008	0.5259(37)	0.65
	0.016	0.5324(28)	0.52
	0.024	0.5400(24)	0.36
	0.032	0.5484(21)	0.27
	0.040	0.5572(19)	0.23
0.3	0.008	0.6304(34)	0.63
	0.016	0.6373(25)	0.56
	0.024	0.6450(21)	0.41
	0.032	0.6532(19)	0.33
	0.040	0.6618(17)	0.29
0.4	0.008	0.7203(32)	0.59
	0.016	0.7275(24)	0.57
	0.024	0.7351(20)	0.44
	0.032	0.7433(18)	0.36
	0.040	0.7518(16)	0.33
0.5	0.008	0.7943(31)	0.64
	0.016	0.8017(23)	0.68
	0.024	0.8095(20)	0.57
	0.032	0.8176(18)	0.50
	0.040	0.8260(16)	0.47

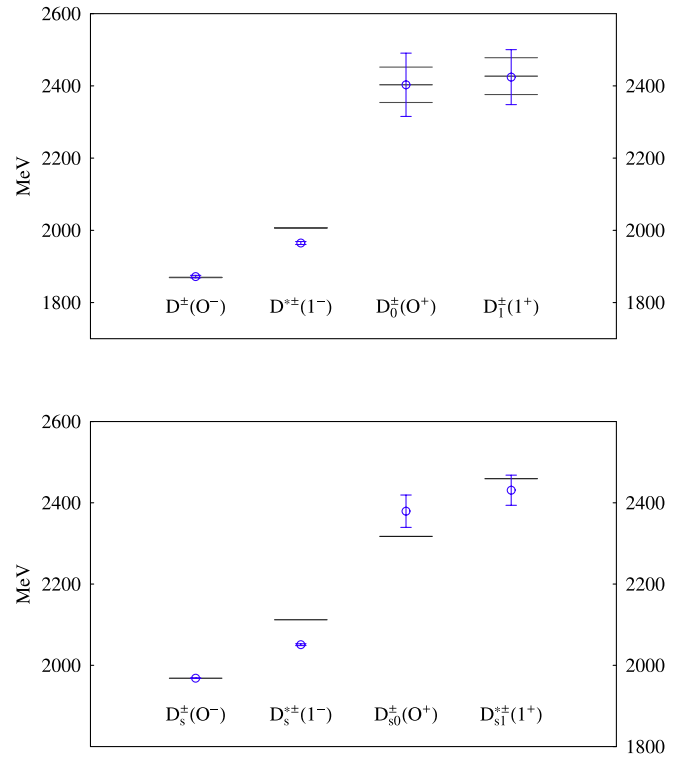
TABLE V. Heavy-light  $J^P = 0^+$  meson mass obtained from fitting to the hyperbolic cosine form in the range of  $10 \leq t \leq 16$ .

$m_{\text{heavy}}$	$m_{\text{light}}$	$m_{\text{PS}}$	$\chi^2$ per d.o.f.
0.2	0.024	0.656(16)	0.01
	0.032	0.654(17)	0.01
	0.040	0.658(10)	0.01
0.3	0.024	0.762(13)	0.02
	0.032	0.760(10)	0.02
	0.040	0.764(8)	0.02
0.4	0.024	0.854(14)	0.01
	0.032	0.853(11)	0.01
	0.040	0.857(9)	0.01
0.5	0.024	0.934(14)	0.01
	0.032	0.932(10)	0.01
	0.040	0.936(8)	0.01

We fit the heavy-light meson mass under a jackknife according to the simple linear form  $m_{Qq} = Am_Q + Bm_q + C$ . We use the pseudoscalar  $D_s$  meson mass [1968.3(5) MeV], the bare strange quark mass estimate of  $am_{\text{strange}} = 0.0298(13)$  [44], and  $\rho$ -meson mass  $m_\rho = 770$  MeV as inputs to determine the bare charm quark mass. The determination using the quarkonium system will be discussed later. For this purpose, we first interpolate the heavy-light pseudoscalar masses in light quark mass to  $am_{\text{strange}}$ , and then interpolate between the resulting data for  $am_{\text{heavy}} = 0.3$  and 0.4. Through this procedure we obtain an estimate of  $am_{\text{charm}}^{D_s/m_\rho} = 0.3583(22)$ , where the superscript denotes the inputs used. Using  $am_{\text{charm}}^{D_s/m_\rho}$ , we estimate the masses of the four different spin-parity states, resulting in Fig. 3, which shows the comparison of our estimates (circles) with the experimental values (vertical lines), and in Table VII. Not surprisingly, the calculations are in reasonable agreement with the experiments, to within a few %.

 TABLE VI. Heavy-light  $J^P = 1^+$  meson mass obtained from fitting to the hyperbolic cosine form in the range of  $10 \leq t \leq 16$ .

$m_{\text{heavy}}$	$m_{\text{light}}$	$m_{\text{PS}}$	$\chi^2$ per d.o.f.
0.2	0.024	0.689(17)	0.004
	0.032	0.688(12)	0.002
	0.040	0.692(10)	0.002
0.3	0.024	0.792(16)	0.011
	0.032	0.790(12)	0.006
	0.040	0.793(10)	0.005
0.4	0.024	0.881(16)	0.017
	0.032	0.879(12)	0.010
	0.040	0.881(9)	0.008
0.5	0.024	0.955(16)	0.02
	0.032	0.952(12)	0.01
	0.040	0.955(9)	0.01


 FIG. 3 (color online). The spectrum of the  $D_s$  (upper panel) and  $D$  (lower panel) systems. The circles are our results with statistical error bars, and the horizontal lines correspond to experimental data with one  $\sigma$  error.

A more stringent test is provided by the parity splittings,  $\Delta_{q,J} = m_{D_q(J^+)} - m_{D_q(J^-)}$ , rather than the masses themselves. The numerical results in physical units via  $a_\rho^{-1}$  are shown in Table VIII together with their experimental values. First we extract some features from the experiments:

- (1)  $\Delta_{q,0} \approx \Delta_{q,1}$  for both  $q = ud$  and  $s$ .
- (2)  $\Delta_{ud,J} > \Delta_{s,J}$  for both  $J = 0$  and 1.
- (3) The difference,  $\Delta_{ud,J} - \Delta_{s,J}$ , is close to  $m_{D_s(J^-)} - m_{D_{ud}(J^-)}$ . This means that the positive parity state masses depend on the mass of the light spectator only weakly while the negative parity states change

TABLE VII. Summary of the heavy-light spectrum (in MeV).

Meson ( $J^P$ )	Experiment	This work
$D^\pm(0^-)$	1869.4(5)	1867(4)
$D^{*\pm}(1^-)$	2010.0(5)	1961(4)
$D_0^{*+}(0^+)$	2352(50)	2401(89)
$D_1^{*+}(1^+)$	2427(26)(25)	2413(76)
$D_s^\pm(0^-)$	1968.3(5)	...
$D_s^{*\pm}(1^-)$	2112.1(7)	2051(2)
$D_{s0}^{*+}(0^+)$	2317.4(9)	2379(40)
$D_{s1}^{*+}(1^+)$	2459.3(1.3)	2431(37)

TABLE VIII. Summary of mass splitting results (in MeV).

	Experiment	This work
$\Delta_{ud,0}$	444(36)	533(90)
$\Delta_{ud1}$	420(36)	452(78)
$1^- - 0^-$	140.64(10)	93(4)
$\Delta_{s,0}$	348.4(9)	411(40)
$\Delta_{s,1}$	345.9(1.2)	380(37)
$1^- - 0^-$	143.8(4)	82(2)

by  $m_{D_s(J^-)} - m_{D_{ud}(J^-)} \approx m_s - m_{ud} \approx m_s$  between  $D_s(J^-)$  and  $D_{ud}(J^-)$ .

There have been attempts to understand some of these features using model analyses. As we noted in the Introduction, Bardeen *et al.* [34] described these charmed heavy-light mesons using a chiral quark model in a way that respected heavy quark symmetry, and predicted that  $\Delta_{q,0} \approx \Delta_{q,1}$  with an assumption that  $\Lambda_{\text{QCD}}/m_{\text{charm}}$  corrections are small. Nowak *et al.* [35] made similar predictions with a slightly different model. Becirevic *et al.* [47] noted difficulties in understanding the experimental observation of  $\Delta_{ud,J} > \Delta_{s,J}$  in terms of a version of chiral perturbation theory extended to include the four spin-parity states of the heavy-light mesons.

Importantly, many previous lattice calculations have systematically overestimated the parity splitting by about 50 to 200 MeV for  $\Delta_{s,0}$  [48–53]. These works are summarized in Fig. 4, which is the same plot given in Ref. [53] but

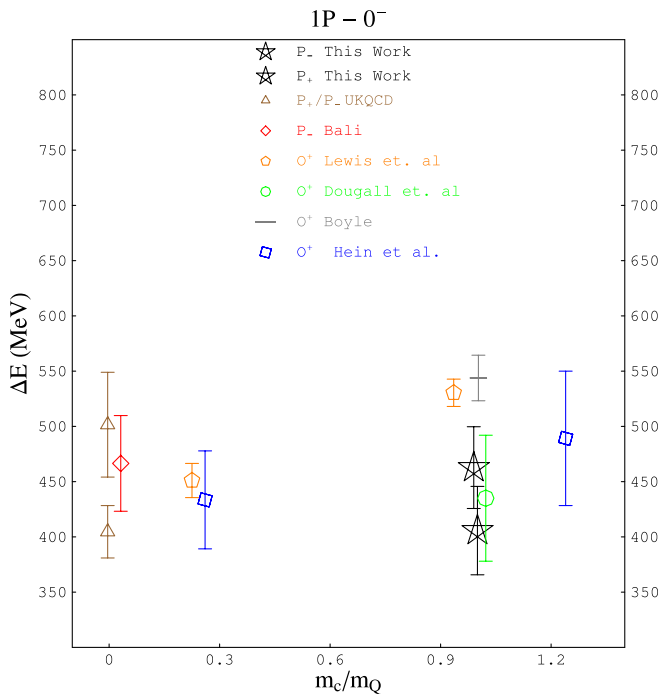


FIG. 4 (color online). The summary plots of the previous lattice estimates for  $\Delta_{s,J}$  including ours.

the results from Dougall *et al.* [52] are modified by applying  $r_0 = 0.50$  fm instead of their 0.55 fm.

Now let us turn to our results. Both  $\Delta_{s,0}$  and  $\Delta_{s,1}$  are overestimated compared with their experimental values by 1–1.5 standard deviations, which corresponds to a difference of 35–60 MeV. Although our results for  $\Delta_{ud,J}$  are not as precise as  $\Delta_{s,J}$  since the extrapolations of the positive parity states to the chiral limit of the light quark suffer from large statistical uncertainty (as described below), they show a consistency with the experimental values. The degeneracy between  $\Delta_{q,0}$  and  $\Delta_{q,1}$  are well reproduced for both  $q = ud$  and  $s$  within the statistical uncertainties. A comparison with the previous lattice calculations is made in Fig. 4. Looking at the data around  $m_c/m_Q = 1$ , the present result obtained at our relatively fine lattice cutoff turns out to be consistent with that of Dougall *et al.* [52], which is obtained in the continuum limit.

The heavy quark mass dependences of  $\Delta_{s,1}$  and  $\Delta_{s,0}$  are shown in Fig. 5 together with the available experimental data. The light quark mass is fixed to the strange quark mass. It is seen that  $\Delta_{s,0}$  and  $\Delta_{s,1}$  are statistically indistinguishable for  $am_{\text{heavy}} > 0.3$ , but that  $\Delta_{s,0} > \Delta_{s,1}$  becomes clearer for smaller  $am_{\text{heavy}}$  as  $\Delta_{s,0}$  increases while  $\Delta_{s,1}$  stays more or less constant. The latter behavior may be supported by the experimental values of the  $K_1(1270)$  and  $K^*(892)$  masses.

The light quark mass dependence of the splittings is shown in Fig. 6, where  $am_{\text{heavy}}$  is fixed to  $am_{\text{charm}}^{D_s/m_\rho}$ . Both  $\Delta_{J=0}$  and  $\Delta_{J=1}$  moderately increase toward lighter quark mass, which is consistent with the experimental observation.

The splitting between the pseudoscalar  $D_s$  and  $D$  mesons,  $m_{D_s} - m_D$ , is calculated to be 101(5) MeV. The central value is slightly above but completely consistent with the experimental value of 99 MeV.

As indicated in Fig. 3, the estimates of the hyperfine splittings are significantly smaller than the experimental

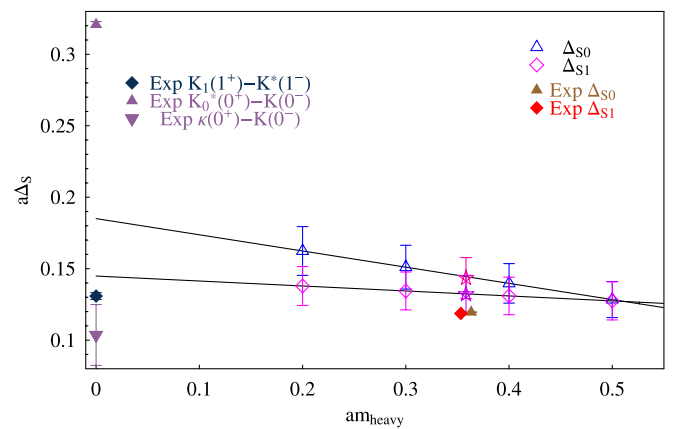


FIG. 5 (color online). The heavy quark mass dependence of parity splitting in lattice units, where  $am_{\text{light}} = am_{\text{strange}}$ . The stars denote  $am_{\text{heavy}} = am_{\text{charm}}$ .

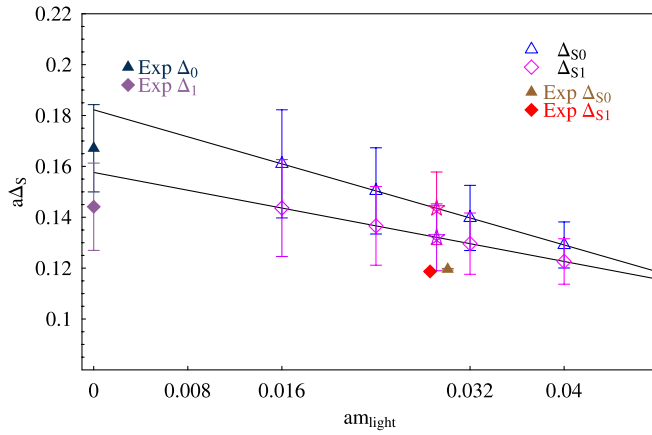


FIG. 6 (color online). The light quark mass dependence of parity splitting in lattice units where  $am_{\text{heavy}} = am_{\text{charm}}^{D_s/m_\rho}$ . The stars denote  $am_{\text{ight}} = am_{\text{strange}}$ .

value. We find the  $1S$  hyperfine splitting  $m_{D^*} - m_D = 93(4)$  MeV and  $m_{D_s^*} - m_{D_s} = 82(2)$  MeV, while the experimental results are 142 and 144 MeV, respectively. This has been a long-standing problem in lattice calculations of heavy quark systems. Take the  $D_s$  system, for example: UKQCD [54] studied the splitting using a nonperturbatively  $O(a)$ -improved Wilson fermion action on quenched Wilson gauge action lattices at  $\beta = 6.2$ , giving  $m_{D_s^*} - m_{D_s} = 95(6)$  MeV using  $m_\rho$  to set the scale. In later studies, Dougall *et al.* [52], using the Sommer scale  $r_0 = 0.55$  fm from the  $K^*/K$  mass ratio, obtained  $m_{D_s^*} - m_{D_s} = 97(6)$  MeV after taking the continuum limit. They also report a result of  $96(2)$  MeV from two-flavor lattices at cutoff  $\approx 1.7$  GeV. Di Pierro *et al.* [50], from  $2 + 1$  staggered dynamical fermion  $20^3 \times 48$ ,  $a \approx 0.13$  fm (from  $r_0 = 0.5$  fm) lattices, report the result  $m_{D_s^*} - m_{D_s} \approx 112(20)$  MeV.

There are many possible reasons for this underestimate in our calculation. Besides the quenched approximation, ambiguity in the lattice spacing, and the light quark mass being extrapolated from rather heavy values to the physical point, one possible reason is the absence of the ‘‘clover term.’’ If one requires accuracy through  $O(a^2 m_{\text{charm}} \Lambda_{\text{QCD}})$  for on-shell quantities, it turns out that one needs to incorporate the clover term into the DWF with proper coefficients [55]. Although naively it is expected that the  $O(a^2 m_{\text{charm}} \Lambda_{\text{QCD}})$  error is fairly small in the present calculation, this needs to be confirmed in future work.

From the above observations, it is interesting to look at the ratio

$$\frac{\Delta_{q,J}}{\Delta_{\text{hyp}}} \quad (2)$$

to see how well a given heavy quark formalism describes the whole heavy-light system. Lattice calculations have overestimated the numerator while underestimating the denominator; thus, obtaining the ratio closer to the experi-

mental value seems to be extremely difficult for any formalism of the lattice heavy quark. In our case, we obtain about 5 for  $am_{\text{heavy}} = 0.4$ , 4 for 0.3, and 3 for 0.2, and presumably any value of the heavy quark mass would not reproduce the experimental value of 2.4 for the charm-strange system. Although we need to take into account the mixing with the other  $0^+$  or  $1^+$  states before a reliable conclusion can be drawn, as  $am_{\text{heavy}}$  becomes smaller, it is worthwhile to keep watching this ratio in future calculations.

## B. Charmonium

The effective mass plots for the four spin-parity channels of the heavy-heavy meson system with  $am_{\text{heavy}} = 0.4$  are shown in Fig. 7. Similarly, good plateaux are observed for other heavy quark masses of 0.1, 0.2, and 0.3. We summarize the meson mass estimates obtained from them in Table IX.

If we interpolate to  $am_{\text{charm}}^{D_s/m_\rho} = 0.3583(22)$  from Sec. III A, we obtain the charmonium mass estimates shown in Table X and Fig. 8, where the experimental values are shown together. Notice that with these inputs the mass of the  $\eta_c$  ( $J^P = 0^-$ ) state is consistent with the experimental value. Alternatively we can get an estimate of  $m_{\text{charm}} = 0.3561(11)$  for the bare charm quark mass from the  $\eta_c$  ( $J^P = 0^-$ ) and  $a_\rho$ . This of course is consistent with the  $am_{\text{charm}}^{D_s/m_\rho}$  estimate.

On the other hand, the calculated hyperfine splitting of  $43(1)$  MeV is significantly smaller than the experimental value of 116 MeV, just like in the charmed-meson cases. One reason for this is what we described in the heavy-light case: that the lack of a clover term might cause the hyperfine splitting to be small. Second, heavy quarkonia hyperfine splittings are notoriously difficult to reproduce by lattice calculations. In the quenched approximation, a detailed study of the relation of hyperfine splitting and the lattice scale was carried out by QCD-TARO Collaboration

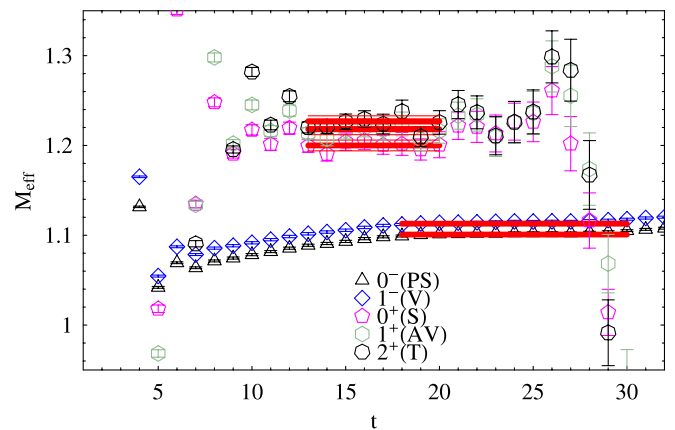


FIG. 7 (color online). Effective mass plots in the heavy-heavy sector at the simulation point  $am_{\text{heavy}} = 0.4$ .

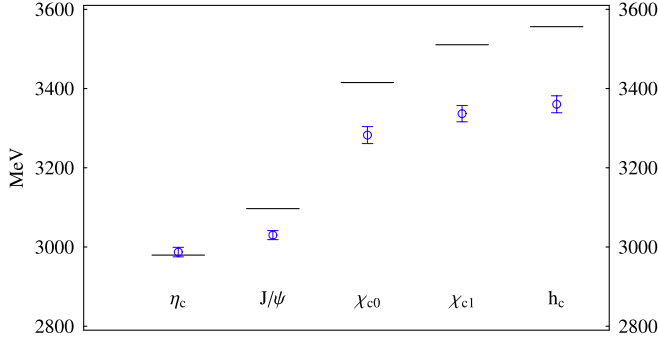


FIG. 8 (color online). The spectrum of the charmonium system. The circles are our results with statistical error bars, and the horizontal lines correspond to experimental values.

[56]. Their result is  $77(2)(6)$  MeV after continuum extrapolation. In the dynamical three-flavor staggered case, S. Gottlieb *et al.* [57] reported their hyperfine splitting to be  $107(3)$  MeV from the “fine” MILC lattice configurations ( $a \approx 0.086$  fm), with the lattice scale obtained from the bottomonium system. In the charmonium system, the problem appears independent of the heavy quark action adopted and is not solved even using dynamical configurations. For more details, see the review article in Refs. [58,59] and the references therein.

The masses of the  $P$ -wave states, in contrast to the charmed-meson cases where they are overestimated, are several standard deviations underestimated from the experimental values.

Also we note a result for the mass of a yet-to-be-established  $C$ -odd axial-vector state,  $h_c(J^{PC} = 1^{+-})$ : experimentally it has been a long-standing puzzle [58]. Recently two positive results with a mass of  $m_{h_c} = 3524.4(6)(4)$  MeV [60,61] and  $3526.2(0.15)(0.2)$  MeV [62] were reported. A third experiment [63], though, did not confirm this. In the present lattice calculation the mass difference between  $h_c$  and  $\chi_{c1}$  is estimated as  $22(11)$  MeV (see Table X). This is obtained from the ratio of the  $h_c$  and  $\chi_{c1}$  correlators in the same fitting range used for extracting the  $\chi_{c0}$  and  $\chi_{c1}$  masses, so it is likely more reliable than the absolute values of the excited-state meson masses themselves. Note these masses are significantly underestimated in the present work. If we add this difference to the experimentally known  $\chi_{c1}$  mass of  $3510.59(10)$  MeV, we get a value of  $3533(11)_{\text{stat}}$  MeV. The  $h_c$  correlator by itself yields  $3361(21)_{\text{stat}}$  MeV. The dominant systematic error contributions are expected to come from the quenched approximation and heavy quark discretizations. MILC Collaboration [64] calculated the quenching effect in charmonium, and their results show agreement in both cases (see Fig. 5 in Ref. [64]) within their statistical error. We would expect the onium to have a small quenching error from individual states but to have an unavoidable discretization error of order  $(am)^2$  (about 10% in our case), giving us  $m_{h_c} = 3361(21)_{\text{stat}}(336)_{\text{sys}}$  MeV.

Finally we discuss the charm mass and lattice cutoff estimations solely by charmonium. First we can determine the bare charm mass by looking at some charmonium mass ratio. For example, if we take a traditional choice of spin-weighted mass ratios,  $[(m_{\chi_{c0}} + 3m_{\chi_{c1}}) - (m_{\eta_c} + 3m_{J/\psi})]/(m_{\eta_c} + 3m_{J/\psi}) = 0.13664(6)$ , we obtain an estimation of  $m_{\text{charm}}a = 0.235(2)$ . Then by matching the experimental mass of  $(m_{\eta_c} + 3m_{J/\psi})/4 = 3.0676(12)$  GeV and the corresponding interpolation of the calculated mass,  $0.804(8) a^{-1}$ , we obtain a cutoff estimate of  $a^{-1} = 3.82(4)$  GeV. If we use spin-0 mesons alone we obtain  $m_{\text{charm}}a = 0.225(2)$  and  $a^{-1} = 3.90(3)$  GeV, and, from spin-1 mesons,  $m_{\text{charm}}a = 0.239(2)$  and  $a^{-1} = 3.79(4)$  GeV. This estimate from charmonium is about 30% larger than the one from  $\rho$  meson mass [44]. The most likely cause of this is of course the quenched approximation. The rectangular improvement of the DBW2 action may also be playing some role here.

### C. Charm quark mass

Presently available estimates of the charm quark mass are given in the PDG review [65]; the charm quark mass is estimated to be in the range

$$1.15 \text{ GeV} \leq m_c^{\overline{\text{MS}}}(m_c) \leq 1.35 \text{ GeV}. \quad (3)$$

The renormalized mass can be obtained from

$$m_{\text{ren}} = Z_m^{\overline{\text{MS}}}(m_f + m_{\text{res}}) \quad (4)$$

where  $Z_m^{\overline{\text{MS}}} = Z^{\text{match}} Z_m^{\text{lat}}$  is the mass renormalization factor between lattice and continuum.  $Z_m^{\text{lat}}$  can be obtained using lattice perturbation theory or the regularization-independent/momentum subtraction (RI/MOM)-scheme nonperturbative renormalization (NPR) either from matching the lattice quark propagator to the continuum one or from the scalar bilinear operator renormalization factor as  $1/Z_S$  [66–68].  $Z^{\text{match}}$  matches between  $\overline{\text{MS}}$  in the continuum and whatever scheme was used on the lattice; the matching between  $\overline{\text{MS}}$  and the RI/MOM scheme can be obtained from Ref. [69]. Aoki *et al.* [70] calculate one-loop  $Z_m^{\overline{\text{MS}}}$  with DWF fermions in the DBW2 gauge action, giving  $Z_m^{\overline{\text{MS}}} = 0.989441$ ; at the scale  $\mu = 2$  GeV it gives  $m_c = 1.0330(64)$  GeV from the  $D_s$  estimate of  $am_{\text{charm}}^{D_s/m_\rho} = 0.3583(22)$ . Chetyrkin calculates the anomalous dimension of the running of the quark mass to  $O(\alpha_s^4)$  [71,72] in the  $\overline{\text{MS}}$  scheme:

$$\mu^2 \frac{d}{d\mu^2} m^{(n_f)}(\mu) = m^{(n_f)}(\mu) \gamma_m^{(n_f)}(\alpha_s^{(n_f)}). \quad (5)$$

The renormalization group invariant mass [73]

$$m_{\text{RI}} = \lim_{\mu \rightarrow \infty} m(\mu) \left[ \frac{33 - 2N_f}{6\pi} \alpha_s \right]^{-12/(33-2N_f)}, \quad (6)$$

TABLE IX. Summary of quarkonium spectrum in lattice units.

$am_{\text{heavy}}$	$0^{-+}$	$1^{--}$	$0^{++}$	$1^{++}$	$1^{+-}$
0.1	0.4614(12)	0.5113(24)	0.604(11)	0.632(9)	0.656(17)
0.2	0.7118(10)	0.7392(14)	0.824(7)	0.848(6)	0.858(8)
0.3	0.9226(8)	0.9406(11)	1.026(6)	1.046(5)	1.053(7)
0.4	1.1008(8)	1.1129(9)	1.200(6)	1.218(6)	1.227(6)
0.5	1.2467(7)	1.2541(8)	1.350(6)	1.364(7)	1.377(5)

TABLE X. Summary of the charmonium spectrum (in MeV). The last row presents a separate estimate on the mass difference between  $h_c$  and  $\chi_{c1}$  obtained directly from the meson propagator ratio: it is likely more reliable than the calculated excited meson masses themselves which are underestimated.

Charmonium ( $J^{PC}$ )	Experiment	This work
$\eta_c(0^{-+})$	2980(1)	2987(12)
$J/\psi(1^{--})$	3096.916(11)	3030(11)
$\chi_{c0}(0^{++})$	3415.19(34)	3282(21)
$\chi_{c1}(1^{++})$	3510.59(12)	3336(21)
$h_c(1^{+-})$	Not established	3360(21)
$h_c - \chi_{c1}$		22(11)

TABLE XI. A list of the past charm quark mass estimations from quenched lattice QCD with continuum extrapolation.

Group	$m_c^{\overline{\text{MS}}}(m_c)$ GeV	Action
Kronfeld [75]	1.33(8)	Clover
Hornbostel <i>et al.</i> [76]	1.20(4)(11)(2)	NRQCD
Becirevic <i>et al.</i> [77]	1.26(4)(12)	Clover
Juge [78]	1.27(5)	Clover
Rolf and Sint [79]	1.301(34)	Clover
de Divitiis <i>et al.</i> [19]	1.319(28)	NRQCD
Nobes <i>et al.</i> [80]	1.22(9)	Fermilab
This work	1.24(1)(18)	DWF

which yields  $m_{\text{RI}} = 1.653(10)$  GeV in our case. The running charm mass is then given by [69,74]

$$m_c(\mu^2) = m_{c,\text{RI}}(\alpha_s)^{4/11} [1 + 0.68733(\alpha_s) + 1.51211(\alpha_s)^2 + 4.05787(\alpha_s)^3]; \quad (7)$$

using  $\alpha_s$  from Eq. (37), we find, at the scale of  $m_c$ , our  $m_c^{\overline{\text{MS}}}(m_c) = 1.239(8)$  GeV. The perturbative renormalization contains a systematic error of  $O(\alpha_s^2) \approx 4\%$ , giving us  $m_c^{\overline{\text{MS}}}(m_c) = 1.24(1)(4)$  GeV. If we start from the charmonium estimate of  $m_c a = 0.235(2)$ , we obtain  $m_c^{\overline{\text{MS}}}(m_c) = 1.07(1)(4)$  GeV. We find that the difference between these two charm quark mass estimates dominates our systematic error; after combining this with the other known systematics, we find the charm quark mass to be 1.24(1)(18).

For the convenience of the reader, some past estimations from quenched lattice QCD with continuum extrapolation are listed in Table XI. Note that UKQCD recently [81] used a two-flavor clover sea to obtain  $m_c^{\overline{\text{MS}}}(m_c) = 1.29(7) \times (13)$  GeV after continuum extrapolation.

#### IV. LEPTONIC DECAY CONSTANTS

The leptonic decay constants are obtained in a standard procedure from two-point correlation functions with heavy-light current  $A_4 = \bar{\Psi}_l \gamma_\mu \gamma_5 \Psi_c$ :

$$\langle 0 | A_4 | \text{PS at rest} \rangle = i f_{\text{PS}} \cdot m_{\text{PS}}. \quad (8)$$

We calculated both  $\mathcal{C}_{\text{pw}}^{A_4 P}$  and  $\mathcal{C}_{\text{ww}}^{PP}$  correlators for pseudo-scalar mesons. Since these two correlators give the same pseudoscalar meson mass ( $m_{\text{PS}}$ ), we can extract  $m_{\text{PS}}$  along with amplitudes from fitting these two correlators simultaneously under a jackknife. That is, we minimize the  $\chi^2$  given by

$$\chi^2 = \sum_{t=t_{\min}}^{t_{\max}} \left\{ \left[ \frac{\mathcal{C}_{\text{pw}}^{A_4 P}(t, 0) - \mathcal{A}_{\text{pw}}^{A_4 P} \sinh(m_{\text{PS}}(t - L_t))}{\sigma_{\text{pw}}^{A_4 P}(t)} \right]^2 + \left[ \frac{\mathcal{C}_{\text{ww}}^{PP}(t, 0) - \mathcal{A}_{\text{ww}}^{PP} \cosh(m_{\text{PS}}(t - L_t))}{\sigma_{\text{ww}}^{PP}(t)} \right]^2 \right\}, \quad (9)$$

where  $\sigma(t)$  is the jackknife error of the correlator at  $t$ . The simultaneous fit gives us more stable amplitudes for two-point correlators than individual fits for the single correlators. The decay constants can be obtained from

$$f_{\text{PS}}^{\text{lat}} = \frac{\mathcal{A}_{\text{pw}}^{A_4 P}}{\sqrt{\frac{m_{\text{PS}}}{2} V \mathcal{A}_{\text{ww}}^{PP}}}, \quad (10)$$

where  $V$  denotes the spatial volume of the lattice.

Booth [82] and Sharpe and Zhang [83] calculate the chiral behavior of the heavy-light decay constants in the quenched approximation to be

$$\sqrt{m_{Qq}} f_{Qq} = F_1 + F_2 m_q + (F_3 m_q + F_4) \ln m_q, \quad (11)$$

after replacement of  $m_{q\bar{q}}^2 \propto m_q$ . McNeile and Michael [84] reported that the effect of the chiral log on  $f_B$  with static light is small. This indicates that we may be able to drop the most divergent term  $\ln m_q$ . To be concrete, we enumerate below various fitting functions that we will use for the purpose of extrapolating/interpolating the light quark mass dependence:

$$\sqrt{m_{Qq}} f_{Qq} = F_1 + F_2 m_q + F_3 m_q \ln m_q, \quad (12)$$

$$\sqrt{m_{Qq}} f_{Qq} = F_1 + F_2 m_q + F_3 m_q^2, \quad (13)$$

$$\sqrt{m_{Qq}} f_{Qq} = F_1 + F_2 m_q, \quad (14)$$

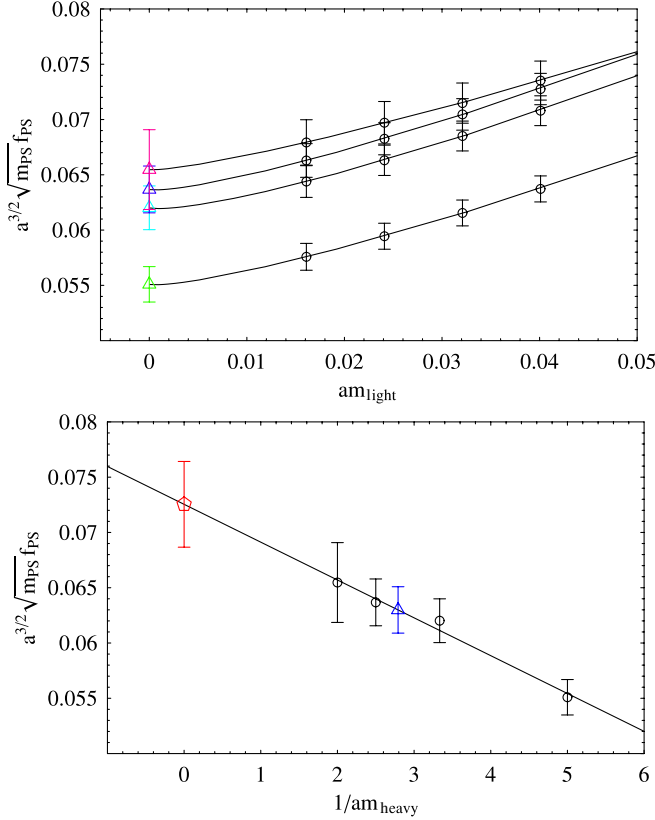


FIG. 9 (color online). The light (upper panel) and heavy (lower panel) quark mass dependence of  $a^{3/2}\sqrt{m_{ps}}f_D$  with the chiral expression  $\sqrt{m_{Qq}}f_{Qq} = F_1 + F_2m_q + (F_3m_q)\ln m_q$  and linear (in  $1/m_{\text{heavy}}$ ) fit, respectively. The top figure displays fixed  $am_{\text{heavy}} \in \{0.2, 0.3, 0.4, 0.5\}$  from top to bottom. In the bottom figure, the triangle (blue) point represents the physical  $D$  meson point,  $0.0688(13)$ , and the pentagon (red) point represents the static quark limit point of  $0.0725(39)$ .

at fixed  $am_{\text{heavy}}$ . Then we examine the  $1/am_{\text{heavy}}$  behavior and interpolate to  $am_{\text{charm}}$ . The upper half of Fig. 9 shows the light quark mass dependence at fixed  $am_{\text{heavy}}$  of the quantity  $\sqrt{m_{Qq}}f_{Qq}$  extrapolated to  $-m_{\text{res}}$  according to Eq. (12), and Fig. 10 shows the light quark mass dependence of the quantity  $\sqrt{m_{Qq}}f_{Qq}$  interpolated to  $m_{\text{strange}}$ . Then we further linearly interpolate (in  $1/M$ ) the heavy quark mass dependence to  $am_{\text{heavy}} = am_{\text{charm}}$ , and summarize the results in Table XII. The results from various expressions used for light quark extrapolation/interpolation are consistent among the fits. Here we take the fit from the quadratic expression, since this falls roughly in the middle of the range from the other expressions, and incorporate the difference from the other fits into the systematic error. Thus, we obtain

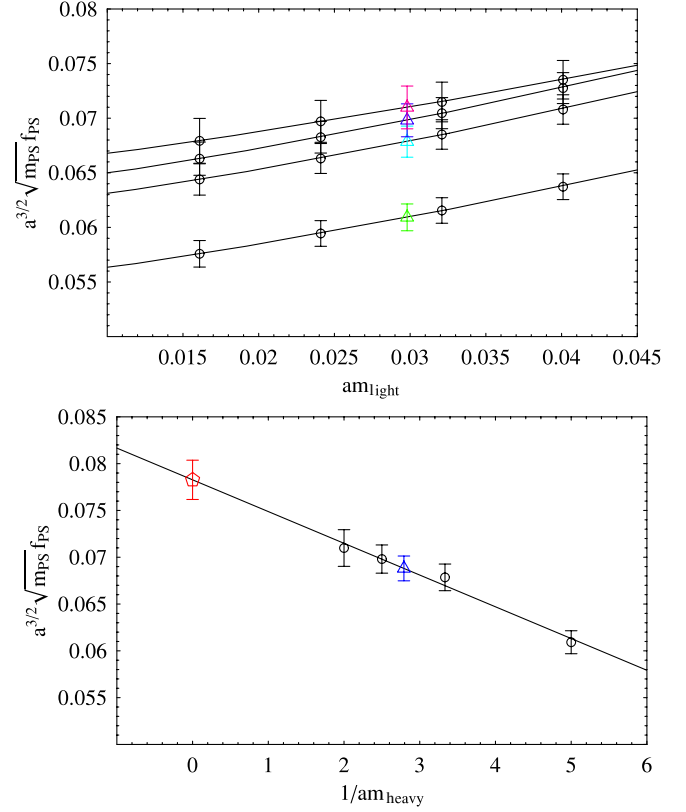


FIG. 10 (color online). The light (upper panel) and heavy (lower panel) quark mass dependence of  $a^{3/2}\sqrt{m_{ps}}f_{D_s}$  with the chiral expression  $\sqrt{m_{Qq}}f_{Qq} = F_1 + F_2m_q + (F_3m_q)\ln m_q$  and linear (in  $1/m_{\text{heavy}}$ ) fit, respectively. In the bottom figure, the triangle (blue) point represents the physical  $D_s$  meson point,  $0.0688(13)$ , and the pentagon (red) point represents the static quark limit point of  $0.0783(21)$ .

$$f_D^{\text{lat}} = 225(7)_{-0}^{(+6)} \text{ MeV}, \quad (15)$$

$$f_{D_s}^{\text{lat}} = 243(4)_{-3}^{(+0)} \text{ MeV}, \quad (16)$$

before renormalization.

In order to compare our lattice calculations with continuum results, we need to properly renormalize our lattice decay constants by a factor of

$$Z_A^{\text{hl}} = Z_A^{\text{ll}} \times \sqrt{\frac{Z_{q,\text{DWF}}(am_{\text{heavy}})}{Z_{q,\text{DWF}}(am_{\text{light}})}}. \quad (17)$$

The nonperturbative light-light current renormalization in the chiral limit,  $m_f = -m_{\text{res}}$ , is calculated in Ref. [44], as  $0.88813(19)$ . Here we employ a quark mass-dependent renormalization factor [55]:

$$Z_{q,\text{DWF}}^{\text{lat}}(am_f, \omega) = \frac{am_f(1 + (am_f)^2) \cosh(m_p^{(0)}) - 2(am_f)^2 \omega \sinh(m_p^{(0)})}{(1 - (am_f)^2) \sinh(m_p^{(0)})}, \quad (18)$$

TABLE XII. Fit expressions and various decay constant related values.

fit	$a^{3/2}\sqrt{m_D}f_D$	$a^{3/2}\sqrt{m_{D_s}}f_{D_s}$	$\frac{\sqrt{m_{D_s}}f_{D_s}}{\sqrt{m_D}f_D}$	$(a^{3/2}\sqrt{m_B}f_B)^{\text{stat}}$	$(a^{3/2}\sqrt{m_{B_s}}f_{B_s})^{\text{stat}}$	$(\frac{\sqrt{m_{B_s}}f_{B_s}}{\sqrt{m_B}f_B})^{\text{stat}}$
$a + bm_q$	0.0621(18)	0.0677(13)	1.090(19)	0.0718(31)	0.0773(25)	1.073(56)
$a + bm_q + cm_q^2$	0.0621(18)	0.0688(13)	1.107(19)	0.0718(31)	0.0783(21)	1.085(37)
$a + bm_q + cm_q \ln m_q$	0.0630(21)	0.0688(13)	1.092(26)	0.0725(39)	0.0783(21)	1.076(53)

in terms of the tree-level on-shell pole mass

$$m_p^{(0)} = \ln \left| \frac{-am_f\omega^2 + \sqrt{(1 + am_f^2)^2 + am_f^2\omega^2(\omega^2 - 4)}}{1 + am_f^2 - 2am_f\omega} \right|, \quad (19)$$

with  $\omega = 2 - M_5$ , and  $Z_{q,\text{DWF}}^{\text{lat}}$  defined as

$$q_R = \sqrt{Z_{q,\text{DWF}}^{\text{lat}}} q_{\text{lat}}. \quad (20)$$

Therefore, the heavy-light current renormalization is 1.0492(22) with  $m_{\text{charm}} = 0.3583(22)$ ; thus  $f_D = 232(7)_{(-6)}^{(+6)}$  and  $f_{D_s} = 254(4)_{(-3)}^{(+3)}$  MeV. Recent experimental measurements for these values are  $f_{D^+} = 222.6 \pm 16.7_{-3.4}^{+2.8}$  MeV [85] and  $f_{D_s} = 267 \pm 33$  MeV [65], and the recent lattice three-flavor dynamical results of MILC and Fermilab [86] are  $f_{D^+} = 201 \pm 3 \pm 17$  MeV and  $f_{D_s} = 249 \pm 3 \pm 16$  MeV.

To calculate the ratio of the decay constants, we first use the chiral form to obtain

$$f_{D_s}\sqrt{m_{D_s}}/f_D\sqrt{m_D} = 1.11(2)_{(-2)}^{(+0)}; \quad (21)$$

Fig. 11 shows an example of our heavy quark mass interpolations of this ratio, with chiral interpolation/extrapolation on the light quark mass according to Eq. (12). We may

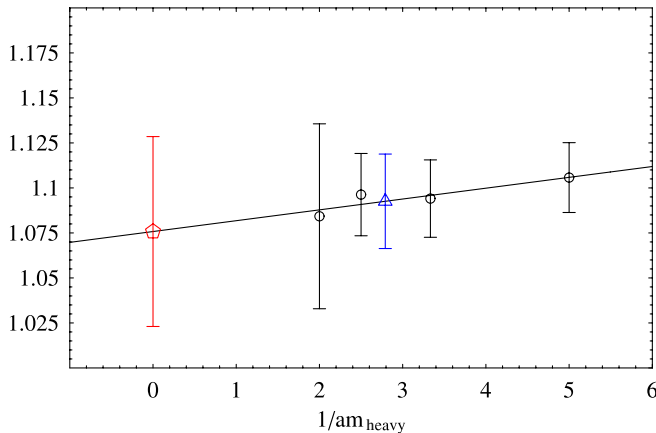


FIG. 11 (color online). The heavy quark mass dependence of the  $SU(3)$  breaking ratio  $\frac{\sqrt{m_{D_s}}f_{D_s}}{\sqrt{m_D}f_D}$  with chiral interpolation/extrapolation [Eq. (12)] in the light quark mass (black points). The triangle (blue) point represents the physical charm quark point, 1.092(26), and the pentagon (red) point represents the static quark limit point of 1.076(53).

then retrieve the ratio of decay constants for the  $D/D_s$  systems by multiplying in appropriate factors of mass

$$f_{D_s}/f_D = 1.05(2)_{(-2)}^{(+0)}. \quad (22)$$

The experimental value suggesting the above ratio is 1.19(25) and the MILC number is 1.24(22). Our result has a smaller central value but agrees with the experimental and dynamical result within one  $\sigma$ .

## V. $D$ - $\bar{D}$ MIXING

In the standard model,  $D^0$ - $\bar{D}^0$  mixing is strongly suppressed by CKM and Glashow-Iliopoulos-Maiani (GIM) factors; if such a mixing is observed, it might be evidence for physics beyond the standard model [87]. The  $D$  mixing is the only probe for the dynamics for the  $c$  quark. The effective Hamiltonian of the QCD contribution to  $\Delta C = 2$  in the standard model comes from the box diagram

$$\mathcal{H}_{\text{eff}}^{\Delta C=2} = \frac{G_F^2}{4\pi^2} |V_{cs}^* V_{cd}|^2 \frac{(m_s^2 - m_d^2)^2}{m_c^2} (\mathcal{O} + 2\mathcal{O}'), \quad (23)$$

where  $\mathcal{O} = \bar{c}\gamma^\mu(1 - \gamma_5)u\bar{c}\gamma_\mu(1 - \gamma_5)u$  and  $\mathcal{O}' = \bar{c}(1 + \gamma_5)u\bar{c}(1 + \gamma_5)u$  result from non-negligible external momentum. The  $b$ -quark contribution is proportional to  $V_{ub}m_b$ , highly suppressed by the very small CKM matrix factor  $V_{ub}$ , which is ignored here. The BABAR  $B$ -factory studies  $D$ - $\bar{D}^0$  mixing from the semileptonic decay modes of  $D^{*+} \rightarrow \pi^+ D^0$  and  $D^0 \rightarrow Ke\nu$  [87]. In this work, we focus on the bag parameter of the  $D$  meson, often defined for historical reasons as

$$B_D = \frac{\langle \bar{D}^0 | \mathcal{O} | D^0 \rangle}{\frac{8}{3} m_D^2 f_D^2}, \quad (24)$$

where  $\mathcal{O} = \bar{c}\gamma^\mu(1 - \gamma_5)u\bar{c}\gamma_\mu(1 - \gamma_5)u$  and  $B_D$  is 1 in the vacuum-insertion approximation.

The parity-even operator for  $B_D$  in the continuum limit is

$$\mathcal{O}_{VV+AA} = (\bar{c}\gamma_\mu u)(\bar{c}\gamma_\mu u) + (\bar{c}\gamma_5\gamma_\mu u)(\bar{c}\gamma_5\gamma_\mu u). \quad (25)$$

However, since DWF does not have exact chiral symmetry,  $\mathcal{O}_{VV+AA}$  mixes with four other operators,

$$\mathcal{O}_{VV-AA} = (\bar{c}\gamma_\mu u)(\bar{c}\gamma_\mu u) - (\bar{c}\gamma_5\gamma_\mu u)(\bar{c}\gamma_5\gamma_\mu u), \quad (26)$$

$$\mathcal{O}_{SS\pm PP} = (\bar{c}u)(\bar{c}u) \pm (\bar{c}\gamma_5 u)(\bar{c}\gamma_5 u), \quad (27)$$

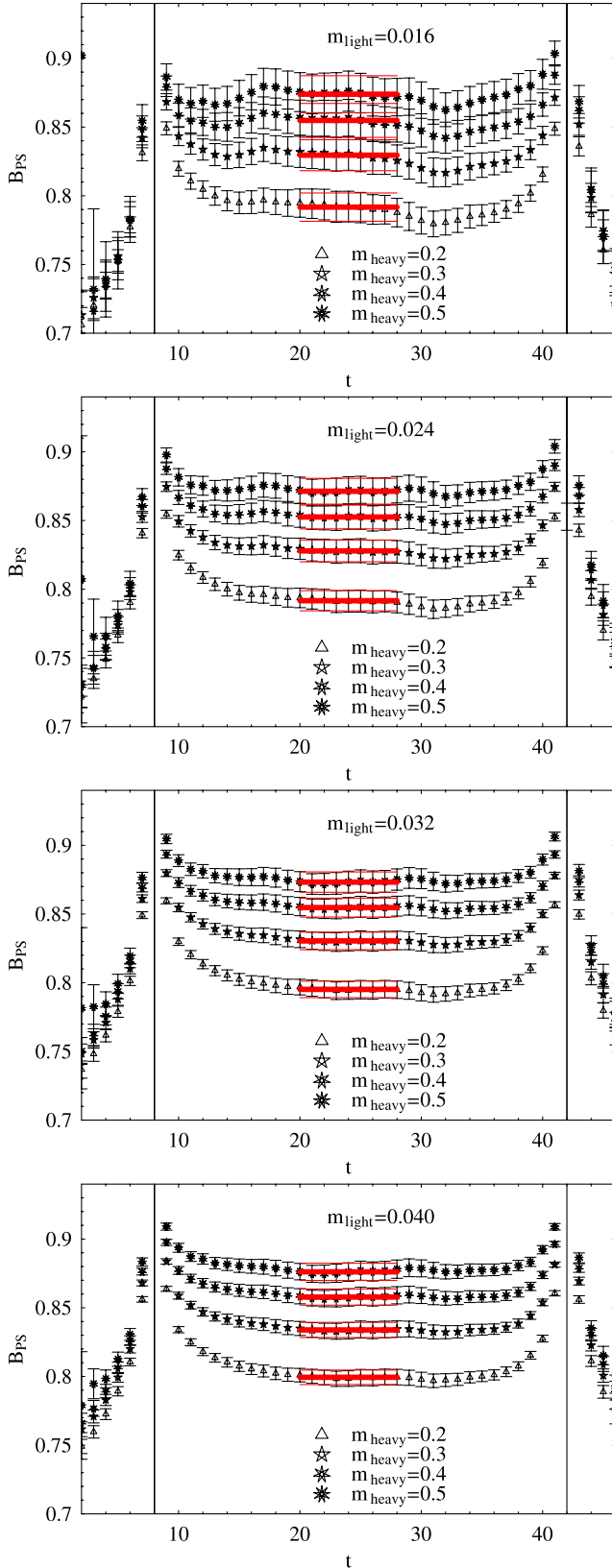


FIG. 12 (color online). The time dependence of pseudoscalar meson bag parameters at fixed light quark mass: 0.016, 0.024, 0.032, 0.040 from top to bottom. In each subgraph, we display the heavy quark mass dependence of  $B_{PS}$ .

$$\mathcal{O}_{TT} = (\bar{c}\sigma_{\mu\nu}u)(\bar{c}\sigma_{\mu\nu}u). \quad (28)$$

The mixing coefficients for these operators do not go to zero as  $m_f$  approaches the chiral limit, but are highly suppressed by  $O((am_{\text{res}})^2)$ , at least in the case for  $B_K$  with DWF. This has been theoretically and numerically demonstrated in Ref. [44], and one can simply ignore the contribution from the above four operators. However, in the finite quark mass region, the correct way of solving this problem is to measure the matrix elements of all the operators in Eqs. (26)–(28) directly on the lattice. These operators are relevant to beyond the standard model sources of mixing in  $\Delta F = 2$  processes [44]. Since we did not do this measurement while the data were taken, we quote the maximal uncertainty from the mixing coefficients, which are expected to be  $O((am_f)^2)$ , due to the soft chiral symmetry breaking from the non-small  $m_f$  term.

On the lattice we can rewrite Eq. (24) directly in terms of the correlation functions obtained on the lattice:

$$B_{PS}^{\text{(lat)}} = \frac{\langle 0 | \chi^\dagger(t_{\text{snk}}) \mathcal{O}(t) \chi^\dagger(t_{\text{src}}) | 0 \rangle}{\frac{8}{3} \mathcal{C}_{\text{pw}}^{A_4 P}(t, t_{\text{snk}}) \mathcal{C}_{\text{pw}}^{A_4 P}(t, t_{\text{src}})} \Big|_{t_{\text{src}} \ll t \ll t_{\text{snk}}}, \quad (29)$$

where  $t_{\text{src}}$  and  $t_{\text{snk}}$  are the source and the sink location of the quarks, and the  $\chi(t)$  are quark bilinear interpolating meson fields. The plateau looks pretty good for extracting the value of  $B_{PS}^{\text{lat}}$ , and details are listed in Table XIII.

Booth [82] and Sharpe and Zhang [83] calculate the chiral behavior of the heavy-light meson bag parameter in the quenched approximation to be

$$B_{Qq} = B_1 + B_2 m_q + B_3 m_q \ln m_q + B_4 \ln m_q. \quad (30)$$

TABLE XIII. List of the  $B_{PS}^{\text{lat}}$  values.

$am_{\text{heavy}}$	$am_{\text{light}}$	$B_{PS}^{\text{lat}}$	$am_{PS}$
0.2	0.016	0.792(10)	0.4839(14)
	0.024	0.792(7)	0.4940(12)
	0.032	0.795(6)	0.5042(11)
	0.040	0.799(5)	0.5146(11)
0.3	0.016	0.830(11)	0.6033(15)
	0.024	0.828(8)	0.6124(13)
	0.032	0.830(6)	0.6218(11)
	0.040	0.834(6)	0.6314(11)
0.4	0.016	0.855(12)	0.7027(15)
	0.024	0.853(9)	0.7113(13)
	0.032	0.855(7)	0.7202(12)
	0.040	0.858(6)	0.7293(11)
0.5	0.016	0.874(13)	0.7865(23)
	0.024	0.871(9)	0.7943(20)
	0.032	0.873(7)	0.8024(18)
	0.040	0.876(6)	0.8110(17)

The coefficient of the most divergent term,  $\ln(m_q)$ , is accompanied by a factor of  $1 - 3g^2$ , where  $g$  is the coupling of  $D - D^* - \pi$  that can be obtained from  $D^* \rightarrow D\pi$  decay [88], which yields a value of 0.2(7). Note that this  $g$  for  $B - B^* - \pi$  is about the same due to heavy quark symmetry. However, it is still hard to judge the effect of this logarithmic dependence in our range of light quark mass. We will ignore it for the rest of paper and incorporate it into the systematic error by comparing with the unquenched calculation, where the  $\ln(m_q)$  term is absent. In order to estimate the systematic error due to our choice of fitting form, we adopt different expressions to extrapolate/interpolate the light quark dependence:

$$B_{Qq} = B_1 + B_2 m_q + B_3 m_q \ln m_q; \quad (31)$$

$$B_{Qq} = B_1 + B_2 m_q + B_3 m_q^2; \quad (32)$$

$$B_{Qq} = B_1 + B_2 m_q. \quad (33)$$

Here we show the extrapolations using Eq. (31) in the

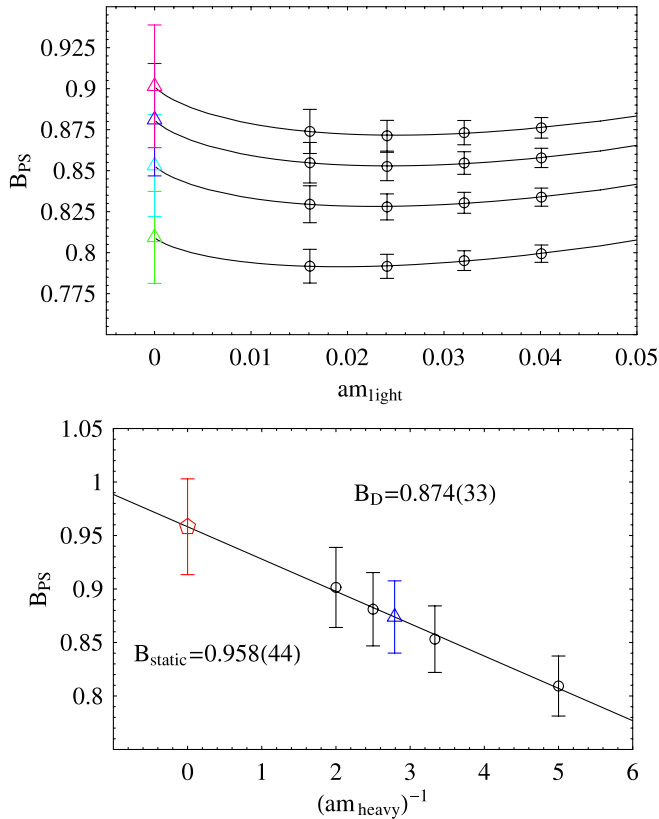


FIG. 13 (color online). The light (upper panel) and heavy (lower panel) quark mass dependence of  $B_{PS}$  with the chiral expression  $B_{Qq} = B_1 + B_2 m_q + B_3 m_q \ln m_q$  and linear (in  $1/M$ ) fit, respectively. The top figure displays light quark mass interpolation to  $-m_{\text{res}}$  at fixed  $am_{\text{heavy}}$ : 0.2, 0.3, 0.4, 0.5 from top to bottom. In the bottom figure, the triangle (blue) point represents the physical  $D$  meson point and the pentagon (red) point represents the static quark limit point.

upper graphs in Fig. 13 to the chiral limit,  $m_f = -m_{\text{res}}$ , and in Fig. 14 to the strange quark mass. The results from various fits are summarized in Table XIV and different analyses agree with each other within statistical error bars. Therefore, we take the quadratic fit as the central value and absorb the other fits into the systematic error; thus we have

$$B_D^{\text{lat}} = 0.859(24)_{-6}^{+24}, \quad (34)$$

$$B_{D_s}^{\text{lat}} = 0.848(7)_{-0}^{+2} \quad (35)$$

before proper renormalization. Note that, since  $D_s$  is a charged meson, there cannot be oscillations between  $D_s$  and  $\bar{D}_s$ . Here we calculate its bag parameter merely for the interest of studying the  $SU(3)$  breaking effect in charmed systems. Also, the extrapolations to the bag parameters from  $B$  and  $B_s$  mesons are simply side products of this study. It is interesting to check the goodness of  $1/M$  extrapolation with the static quark lattice studies.

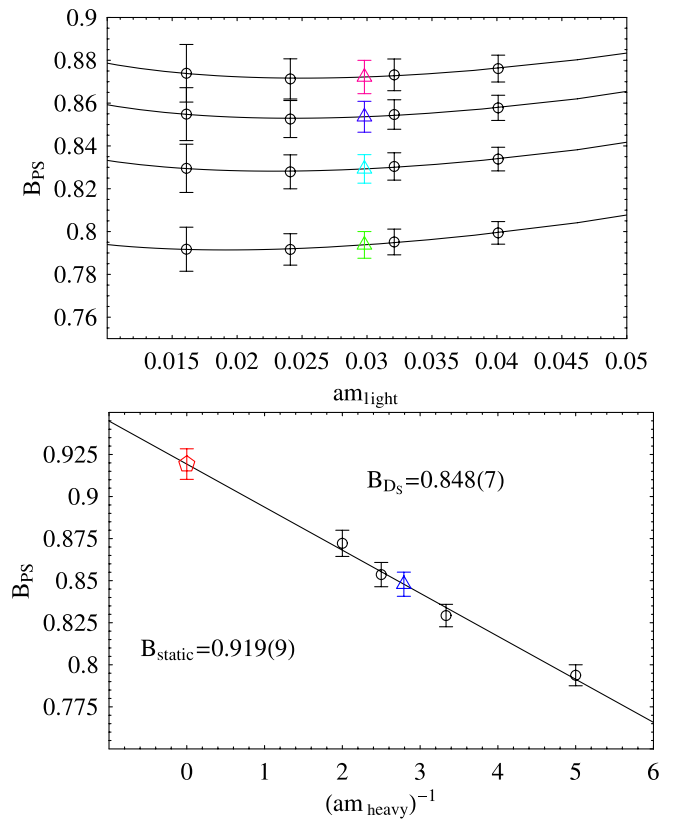


FIG. 14 (color online). The light (upper panel) and heavy (lower panel) quark mass dependence of  $B_{PS}$  with the chiral expression  $B_{Qq} = B_1 + B_2 m_q + B_3 m_q \ln m_q$  and linear (in  $1/M$ ) fit, respectively. The top figure displays light quark mass interpolation to  $m_{\text{strange}}$  at fixed  $am_{\text{heavy}}$ : 0.2, 0.3, 0.4, 0.5 from top to bottom. In the bottom figure, the triangle (blue) point represents the physical  $D_s$  meson point and the pentagon (red) point represents the static quark limit point.

TABLE XIV. Fit expressions and various bag parameter values.

Fit	$B_D$	$B_{D_s}$	$B_{D_s}/B_D$	$(B_B)^{\text{static}}$	$(B_{B_s})^{\text{static}}$	$(B_{B_s}/B_B)^{\text{static}}$
$a + bm_q$	0.845(16)	0.849(8)	1.001(12)	0.923(22)	0.921(10)	0.998(14)
$a + bm_q + cm_q^2$	0.859(24)	0.848(7)	0.987(22)	0.940(33)	0.919(9)	0.977(28)
$a + bm_q + cm_q \ln m_q$	0.874(33)	0.848(7)	0.970(32)	0.958(45)	0.919(9)	0.959(39)

We take advantage of the bag parameter NPR done in Ref [44] with the RI/MOM scheme and further convert into  $\overline{\text{MS}}$ . References [89,90] calculated the conversion factors in next-to-leading-order perturbation theory. First, we convert the renormalization factor into an RI value

$$Z_B^{\text{RI}} = [\alpha_s(\mu^{\text{lat}})]^{-2/l} \left[ 1 + \frac{\alpha_s(\mu^{\text{lat}})}{4\pi} J_{\text{RI/MOM}} \right] \times Z_B^{\text{lat,RI/MOM}}(\mu^{\text{lat}}), \quad (36)$$

where

$$\alpha_s(\mu) = \frac{12\pi}{(33 - 3N_f) \ln(\mu^2/\Lambda_{\text{QCD}}^2)} \times \left( 1 - \frac{918 - 90N_f - 24N_f^2}{(33 - 2N_f)^2} \frac{\ln \ln(\mu^2/\Lambda_{\text{QCD}}^2)}{\ln(\mu^2/\Lambda_{\text{QCD}}^2)} \right), \quad (37)$$

with  $N_f = 0$ , and  $\Lambda_{\text{QCD}}^0 = 238$  MeV and  $J_{\text{RI/MOM}}(N_f = 0) = 2.883$ ; that gives  $Z_B^{\text{RI}} = 1.409(5)$ . Then we calculate the factor for  $N_f = 4$ , as

$$Z_B^{\overline{\text{MS}}} = \alpha_s(\mu)^{25/3} \left[ 1 + \frac{\alpha_s(\mu^{\text{lat}})}{4\pi} J_{\overline{\text{MS}}} \right]^{-1} \hat{Z}_B. \quad (38)$$

The  $\Lambda_{\text{QCD}}$  with  $N_f = 5$  is 217 MeV [65], suggesting that the  $\Lambda_{\text{QCD}}$  is 276 MeV for  $N_f = 4$ . Then  $\alpha_s(\mu = 2 \text{ GeV})$  is 0.283. Therefore,  $Z_B^{\overline{\text{MS}}}$ , is 1.000(4) and our bag parameters are

$$B_D = 0.845(24)_{(-6)}^{(+24)}, \quad (39)$$

$$B_{D_s} = 0.835(7)_{(-0)}^{(+2)}, \quad (40)$$

$$B_{D_s}/B_D = 0.987(22)_{(-27)}^{(+0)}. \quad (41)$$

## VI. $SU(3)$ BREAKING RATIOS

In the long run, lattice QCD should provide a high-precision determination of  $SU(3)$  flavor breaking of the  $\Delta F = 2$  heavy-light matrix element

$$\frac{\mathcal{M}_{Qs}}{\mathcal{M}_{Ql}} = \frac{\langle \bar{P}_{Qs} | \bar{Q} \gamma_\mu (1 - \gamma_5) s \bar{Q} \gamma_\mu (1 - \gamma_5) s | P_{Qs} \rangle}{\langle \bar{P}_{Ql} | \bar{Q} \gamma_\mu (1 - \gamma_5) l \bar{Q} \gamma_\mu (1 - \gamma_5) l | P_{Ql} \rangle}, \quad (42)$$

where  $Q$  stands for heavy quark,  $l$  stands for light quark ( $u, d$ ), and  $P_{Ql}$  represents a pseudoscalar meson composed of  $Q$  and  $l$ . There are two ways of obtaining this ratio: first, by calculating the matrix element directly [91]; second, by calculating the decay constants and bag parameters separately and combining them with Eq. (24). In this work, we will focus on the second method (often referred to as the ‘‘indirect’’ approach) to get the ratios by the combination of ratios of bag parameters and decay constants:

$$r_Q = \frac{\mathcal{M}_{Qs}}{\mathcal{M}_{Ql}} = \frac{B_{Qs}(m_{Qs}f_{Qs})^2}{B_{Ql}(m_{Ql}f_{Ql})^2}. \quad (43)$$

Therefore, it is important to obtain the ratio of

$$\frac{f_{Qs}}{f_{Ql}} \sqrt{\frac{B_{Ql}}{B_{Qs}}} = \xi_Q. \quad (44)$$

Table XV summarizes  $\xi_Q$  and the  $SU(3)$  breaking for different chiral extrapolation formulas. From the charm quark sector, we obtain

$$\xi_c = 1.071(23)_{(-31)}^{(+0)} \quad (45)$$

and

$$r_c = 1.273(65)_{(-67)}^{(+0)}. \quad (46)$$

## VII. EXTRAPOLATION TO STATIC $B$ MESONS

Although our main goal in this work is to apply the DWF to the charm quark physics directly, it is of some interest to extrapolate the heavy quark mass to the static limit. In the

TABLE XV. Fit expressions and various bag parameter values.

Fit	$\frac{f_{D_s}}{f_D} \sqrt{\frac{B_{D_s}}{B_D}}$	$\left(\frac{f_{D_s} m_{D_s}}{m_D f_D}\right)^2 \frac{B_{D_s}}{B_D}$	$\frac{f_{B_s}}{f_B} \sqrt{\frac{B_{B_s}}{B_B}}$	$\left(\frac{f_{B_s} m_{B_s}}{m_B f_B}\right)^2 \frac{B_{B_s}}{B_B}$
$a + bm_q$	1.064(29)	1.257(73)	1.019(53)	1.27(13)
$a + bm_q + cm_q^2$	1.071(23)	1.273(65)	1.019(37)	1.274(94)
$a + bm_q + cm_q \ln m_q$	1.048(31)	1.219(80)	1.001(53)	1.23(13)

past, as is pointed out in Refs. [92,93], some static limit  $B$  parameters obtained from extrapolation from the charm region with simple linear function in  $1/m_{\text{heavy}}$  were found to disagree with direct static calculations: after all, the charm mass may not be sufficiently heavy to justify such a simple extrapolation to the static limit. However, as a mere by-product of our work on charm, the extrapolation may still be instructive.

### A. Decay constants

Since we do not know how to renormalize the heavy-light decay constant for a static quark with DWF as the light quark action, we will only focus on ratios of decay constants. Since the bottom quark is so heavy compared to the scale of our physics, we may extrapolate to the static quark limit to get the result pertaining to  $B$  mesons. The ratio is

$$(f_{B_s} \sqrt{m_{B_s}} / f_B \sqrt{m_B})^{\text{static}} = 1.08(4)({}_{-2}^{+1}). \quad (47)$$

Taking  $m_{B_s}/m_B$  as 1.017 [65], we have

$$(f_{B_s}/f_B)^{\text{static}} = 1.06(4)({}_{-2}^{+1}). \quad (48)$$

A previous quenched study using the static approximation for the heavy fermion action and the step-scaling technique [94] gives 1.11(16) when extrapolated to the continuum limit, which is consistent with our extrapolation result here. A recent study using partially quenched two-flavor DWF lattices with the static approximation [95] (with lattice cutoff  $\approx 1.7$  GeV) yields 1.29(4)(4)(2) for the same quantity, giving us an idea of the systematic error due to the quenched approximation. HPQCD uses a 2 + 1 staggered fermion sea with NRQCD heavy quark action and lattice cutoffs  $\approx 1.6$  GeV and  $\approx 2.6$  GeV to obtain the ratio 1.20(2)(1) [96].

### B. Bag parameters

Following the analyses in Sec. V, we extrapolate lattice bag parameters to the static limit,

$$(B_B^{\text{lat}})^{\text{static}} = 0.940(33)({}_{-6}^{+30}), \quad (49)$$

$$(B_{B_s}^{\text{lat}})^{\text{static}} = 0.919(9)({}_{-0}^{+3}). \quad (50)$$

We set the scale  $\mu$  at the mass of the  $b$  quark, 4.5 GeV, and the renormalization factor  $Z_B^{\overline{\text{MS}}}(m_b)$  (with  $N_f = 5$ ) is 0.920(3), which suggests

$$(B_B)^{\text{static}} = 0.865(33)({}_{-6}^{+30}), \quad (51)$$

$$(B_{B_s})^{\text{static}} = 0.845(9)({}_{-0}^{+3}). \quad (52)$$

Reference [97] uses static heavy and Wilson light quark actions to get  $B_B(m_b) = 0.98(4)({}_{-18}^{+3})$  at the  $\approx 1.8$  GeV

lattice cutoff. Another quenched study with static heavy and overlap light quarks gives [98] (again, with the finest lattice cutoff  $\approx 1.8$  GeV)

$$(B_{B_s}(m_b))^{\text{static}} = 0.940(16)(22). \quad (53)$$

Our number does not agree too well with previous static results. This might be due to the coarse lattices used in their simulations. However, our number agrees better with JLQCD's quenched calculation with NRQCD [99], where the finest lattice spacing is 2.3 GeV:

$$B_{B_d}(m_b) = 0.84(3)(5), \quad (54)$$

$$B_{B_s}/B_{B_d} = 1.020(21)({}_{-16}^{+15})({}_{-0}^{+5}), \quad (55)$$

$$B_{S_s}(m_b) = 0.85(1)(5)({}_{-0}^{+1}), \quad (56)$$

after taking the continuum limit. Our results for the  $B$  case are consistent with the two-flavor DWF static-light calculation in Ref. [95]:

$$(B_B)^{\text{static}} = 0.812(48)(67)({}_{-300}^{+0}), \quad (57)$$

$$(B_{B_s})^{\text{static}} = 0.864(28)(71)({}_{-320}^{+0}), \quad (58)$$

$$(B_{B_s}/B_B)^{\text{static}} = 1.06(6)(3)(1), \quad (59)$$

and the two-flavored  $O(a)$ -improved Wilson fermion sea with NRQCD heavy quark study [100] done by JLQCD,

$$(B_B) = 0.836(27)({}_{-62}^{+56}), \quad (B_{B_s}/B_B) = 1.017(16)({}_{-17}^{+56}). \quad (60)$$

### C. $SU(3)$ breaking ratio

Extending the discussions in Sec. VI, we have the results for the bottom sector:  $\xi_b = 1.019(37)({}_{-34}^{+16})$  and the  $SU(3)$  breaking ratio  $r_b = 1.274(94)({}_{-180}^{+32})$ . It is useful to recall that in the first calculation in Ref. [91], using a Wilson fermion action,  $\xi_b = 1.30(4)({}_{-15}^{+21})$  and  $1.17(2)({}_{-6}^{+12})$  were found after linear continuum extrapolations from direct and indirect methods, respectively. A previous static quark study on a two-flavor DWF sea gives  $\xi_b = 1.33(8)(8)$  [95]. Using JLQCD's ratio of bag parameters [100] and HPQCD's 2 + 1 result [86] on decay constants, the Lattice '05 review [101] gives  $\xi_b = 1.210({}_{-35}^{+47})$  and the previous world average [102] gives  $\xi_b = 1.23(6)$ . Our central value is smaller than these previous results but quite consistent with other studies given our relatively large errors. We first take the light quark mass limit according to the heavy-light meson bag parameter chiral formula and then take the heavy quark mass to  $m_{\text{charm}}^{\text{lat}}$ ; Figs. 13 and 14 show that the chiral behavior of the light

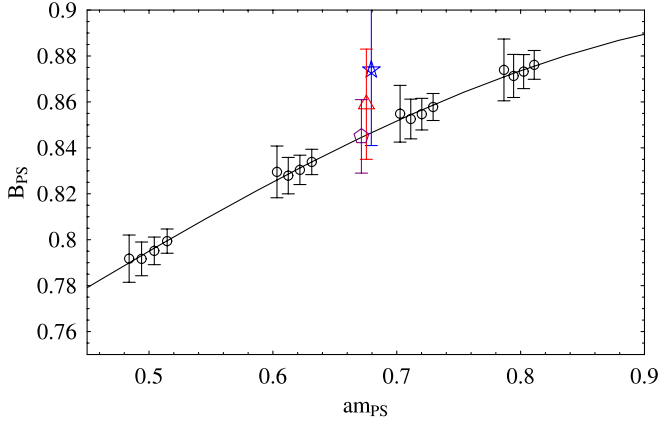


FIG. 15 (color online). The  $B_{\text{PS}}^{\text{lat}}$  as a function of the pseudo-scalar meson. The circle points are the data points and the black line is the fit of the form  $B_{\text{PS}}(m_{\text{PS}}) = B_1 + B_2 m_{\text{PS}}^2 + B_3 m_{\text{PS}}^2 \ln m_{\text{PS}}^2$ . The star (blue) point is the  $B_D^{\text{lat}}$  point obtained from Fig. 13, the triangle (red) point is the  $B_D^{\text{lat}}$  from the quadratic fit, and the pentagon (purple) point is the  $B_D^{\text{lat}}$  from the linear fit.

quark part makes the bag parameters for mesons with up and down quarks somewhat larger than those with a strange quark. However, the other studies get their bag parameters by fitting the bag parameter as a function of heavy-light pseudo-scalar mass, instead of the heavy-light chiral forms; see the dependence for our data in Fig. 15. The bag parameter increases with the pseudo-scalar mass. Therefore, if one fits the bag parameter function as input of heavy-light pseudo-scalar mass, from a relation  $m_{\{B,D\}_s}/m_{\{B,D\}} > 1$ , which always holds, it follows that  $B_{\{B,D\}_s}/B_{\{B,D\}} > 1$ . Therefore,  $\xi_Q$  in these studies must come out larger than our values.

## VIII. SYSTEMATIC ERRORS

The systematic errors on the charmonium system have been discussed in their own subsections. In this section, we will focus on the systematic error on bag parameters and decay constants. In the previous sections, we presented our calculation with statistical errors computed using the jack-knife procedure, along with systematic errors mostly caused by chiral extrapolation. There are other potential sources of systematic errors caused by the quenched approximation: finite-volume effects, operator mixing and matching calculations. Here is a detailed estimate of the various systematic errors.

### (i) Finite volume

The proper way to estimate this error is to perform the calculation on at least two different volumes and extrapolate to the infinite-volume limit. However, in this work, we only perform our calculation in one lattice volume, which is about  $(1.6 \text{ fm})^3$ . Since the scale of the  $D$  system is in between  $K$  and  $B$ , we will estimate our finite-volume error by quoting which-

ever system ( $K$  or  $B$ ) has a larger finite-volume error in previously published studies. Reference [44], which uses the same lattice box we do, quoted a 2% error in  $B_K$  by comparing with a 2.4 fm box. We also compare our  $B_B$  found by extrapolation to the static limit with a quenched, larger-volume ( $\approx 2.4 \text{ fm}$ ) calculation [99], which gives  $B_{B_d}(m_b) = 0.84(3)(5)$  with NRQCD fermions; this gives us an estimation of 0.4% error. Taking the larger of these two estimates, we conclude that the finite-volume effect on the  $B_D$  should be smaller than 2%.

### (ii) Continuum extrapolation

In this paper, we only perform our calculation at one lattice spacing, and therefore we cannot extrapolate our result to the continuum limit. This should be checked carefully in future works. The next-best thing we can do is to estimate the error from a continuum extrapolation study from the same gauge configuration. Such a study has been performed on the decay constants and matrix elements of the  $K$  system in Ref. [44] with an additional lattice cutoff at 1.982(30) GeV. The result shows mild dependence from  $a^{-1} \approx 3 \text{ GeV}$  to the continuum. Therefore, we add 0.2% to our systematic errors due to continuum extrapolation.

### (iii) RI formulation

We need the  $\alpha_s$  to first convert the scale-dependence RI/MOM NPR factor,  $Z_B^{\text{RI/MOM}}$ , to an RI value and further convert it to an  $\overline{\text{MS}}$  one. In the expression, we use the next-to-leading-order formulation, which leaves the remaining leading error up to  $O(\alpha_s^2) \approx 4\%$ .

### (iv) NPR renormalization factor in bag parameters

We adopt the RI/MOM NPR renormalization factor from Ref. [44], and we quote the estimation within that paper as 1%.

### (v) Operator mixing

We have discussed mixing with wrong-chirality operators, which contributes around 10% uncertainty to our final  $B_D$  calculation.

### (vi) Quenched approximation

The quenched approximation ignores sea quark loop contributions which, in general, are considered to be a major contribution to systematic errors. Reference [44], which uses the same quenched lattice ensemble as in the present work, quotes a 6% error on the  $B_K$  factor due to this approximation, after comparing with the number calculated on two-flavor DWF lattices. Similarly, we can compare our static quark limit value with the one calculated on two-flavor DWF lattices [95], which gives us 6%. Therefore, it seems reasonable to use a 6% systematic quenching error for  $B_D$  as well.

The above discussions mainly focus on the matrix elements. A similar estimation is also applied to the decay

constants, except for operator mixing issues. Thus, we expect about 7.5% error on the decay constants.

## IX. CONCLUSION

In this work, we use the DWF formulation for charm quarks as well as the three lighter flavors, up, down and strange, on the lattice with a relatively high cutoff (around 3 GeV). We use the mass ratio  $m_K/m_\rho$  to set the bare strange quark mass  $m_{\text{strange}}a = 0.0298(13)$  in lattice units. Then combining this and another hadronic mass ratio  $m_{D_s}/m_\rho$  we obtain the bare charm mass,  $m_{\text{charm}}a = 0.3583(22)$ .

Using the bare quark mass values that we found, we conclude the following for charmed and charmed-strange meson states:

- (i) The masses of the  $J^P = 0^\pm$  and  $1^\pm$   $D$ ,  $D^*$ ,  $D_s$  and  $D_{sJ}$  states are well reproduced to within a few percent.
- (ii) Their parity splittings,  $\Delta_J$ , are better reproduced than in previous works, with only 10%–20% over estimations.
- (iii) The experimental observation of  $\Delta_{ud} > \Delta_s$  is reproduced.
- (iv) The hyperfine splittings are only 60%–65% reproduced.

Regarding the dependence on heavy quark mass,

- (i)  $\Delta_{J=0}$  and  $\Delta_{J=1}$  are degenerate for  $m_{\text{heavy}}a > 0.2\text{--}0.3$ .
- (ii)  $\Delta_{J=0}$  increases as  $m_{\text{heavy}}$  decreases further, while
- (iii)  $\Delta_{J=1}$  does not.

Also with the bare charm quark mass we worked out the renormalization factor,  $Z_m$ , from the existing one-loop domain-wall perturbation calculation. After RI scaling,  $m_c^{\overline{\text{MS}}}(m_c) = 1.239(8)$  GeV. After consideration of systematic errors from the perturbative renormalization and bare quark mass shift, we have  $m_c^{\overline{\text{MS}}}(m_c) = 1.24(1)_{\text{stat}} \times (18)_{\text{syst}}$  GeV.

In the charmonium system we find the  $\eta_c$  mass agrees well with the experimental value. The  $J/\psi$  mass (hence the hyperfine splitting) is smaller than the experimental one, confirming the long puzzle in lattice QCD. We also note a prediction for the mass of the yet-to-be-discovered  $C$ -odd  $h_c$  state: the mass difference between  $h_c$  and  $\chi_{c1}$  is estimated as  $22(11)$  MeV. This would translate to the mass of  $3533(11)_{\text{stat}}(336)_{\text{syst}}$  MeV for this meson.

The leptonic decay constants are also calculated. We tried to estimate the systematic uncertainty from the associated quenched logarithm by adopting three different fitting formulations. Our result, after considering other

systematic uncertainties due to the quenched approximation and continuum extrapolation, gives us

$$f_D = 232(7)_{\text{stat}}({}_{-0}^{+6})_{\text{chiral}}(17)_{\text{syst}} \text{ MeV}, \quad (61)$$

$$f_{D_s}/f_D = 1.05(2)_{\text{stat}}({}_{-2}^{+0})_{\text{chiral}}(2)_{\text{syst}}. \quad (62)$$

We also discussed extrapolation to the static limit in terms of  $1/m_{\text{heavy}}$  which gives results consistent with previous static calculations.

The bag parameters of the  $D$  and  $D_s$  (purely theoretical but interesting in regards to the  $SU(3)$  breaking effect) are studied. The use of domain-wall fermions on the current fine lattice with only softly broken chiral symmetry gives us some advantages such as the absence of complicated mixing and the availability of the RI/MOM nonperturbative renormalization techniques. We include a detailed estimation of systematic uncertainties. The biggest systematic errors come from the quenched approximation and the mixing of wrong-chirality operators. Our result is

$$B_D(2 \text{ GeV}) = 0.845(24)_{\text{stat}}({}_{-6}^{+24})_{\text{chiral}}(105)_{\text{syst}}, \quad (63)$$

$$B_{D_s}/B_D = 0.987(22)_{\text{stat}}({}_{-27}^{+0})_{\text{chiral}}(23)_{\text{syst}}, \quad (64)$$

where the first error is statistical, the second is systematic from fitting, and the third combines all other known systematics. Thus a minor  $SU(3)$  breaking is seen in our calculation. We also discussed extrapolation to the static limit in terms of  $1/m_{\text{heavy}}$  which suggests the  $D$  and  $D_s$  meson results are reliable.

In conclusion, using DWF to simulate the charm quark on a quenched ensemble at a moderately high cutoff of about 3 GeV obtained with the DBW2 action results in reasonable descriptions for most of the calculated meson observables: the masses and their splittings, the leptonic decay constant, and  $\Delta C = 2$  mixing. It seems the charm quark propagation is successfully described with the current setup. This obviously is an attractive direction to proceed in, especially with dynamical QCD ensembles that are becoming available.

## ACKNOWLEDGMENTS

We thank Junichi Noaki for generating the gauge configurations and for useful discussions, various RBC members for physics discussions, and RIKEN, Brookhaven National Laboratory and the U.S. Department of Energy for providing the facilities essential for the completion of this work. N. Yamada is supported in part by the Grant-in-Aid of the Ministry of Education (No. 18034011, No. 18340075, No. 18740167). H.-W. Lin is supported by DOE Grant No. DE-FG02-92ER40699. A. Soni is supported in part by DOE Grant No. DE-AC02-98CH10886.

- [1] G. Bonvicini *et al.* (CLEO Collaboration), *Phys. Rev. D* **70**, 112004 (2004).
- [2] K. Arms *et al.* (CLEO Collaboration), *Phys. Rev. D* **69**, 071102 (2004).
- [3] B. I. Eisenstein *et al.* (CLEO Collaboration), hep-ex/0408055.
- [4] D. Besson *et al.* (CLEO Collaboration), *AIP Conf. Proc.* **698**, 497 (2004).
- [5] K. T. Flood (BABAR Collaboration), *Int. J. Mod. Phys. A* **20**, 3686 (2005).
- [6] B. Aubert *et al.* (BABAR Collaboration), *Phys. Rev. Lett.* **90**, 242001 (2003).
- [7] L. Benussi (FOCUS Collaboration), *Int. J. Mod. Phys. A* **20**, 549 (2005).
- [8] M. Danilov (Belle Collaboration), in *Proceedings of the 32nd International Conference on High-Energy Physics (ICHEP 04), Beijing, China, 2004*, edited by Hesheng Chen, Dongsheng Du, Weiguo Li, and Caidian Lu (World Scientific, Singapore, 2004).
- [9] K. Abe *et al.*, hep-ex/0507019.
- [10] A. Drutskoy *et al.* (Belle Collaboration), *Phys. Rev. Lett.* **94**, 061802 (2005).
- [11] E. Swanson, *AIP Conf. Proc.* **814**, 203 (2006); *Int. J. Mod. Phys. A* **21**, 733 (2006).
- [12] C. Quigg, *Proc. Sci.*, HEP2005 (2006) 400 [hep-ph/0509327].
- [13] T. Barnes, *AIP Conf. Proc.* **814**, 735 (2006).
- [14] E. Eichten and B. Hill, *Phys. Lett. B* **234**, 511 (1990).
- [15] E. Eichten and B. Hill, *Phys. Lett. B* **240**, 193 (1990).
- [16] E. Eichten and B. Hill, *Phys. Lett. B* **243**, 427 (1990).
- [17] B. A. Thacker and G. P. Lepage, *Phys. Rev. D* **43**, 196 (1991).
- [18] G. P. Lepage, L. Magnea, C. Nakhleh, U. Magnea, and K. Hornbostel, *Phys. Rev. D* **46**, 4052 (1992).
- [19] G. M. de Divitiis, M. Guagnelli, R. Petronzio, N. Tantalo, and F. Palombi, *Nucl. Phys.* **B675**, 309 (2003).
- [20] G. M. de Divitiis, M. Guagnelli, F. Palombi, R. Petronzio, and N. Tantalo, *Nucl. Phys.* **B672**, 372 (2003).
- [21] A. Juttner and J. Rolf (ALPHA Collaboration), *Phys. Lett. B* **560**, 59 (2003).
- [22] H.-W. Lin and N. H. Christ, *Proc. Sci.*, LAT2005 (2006) 225 [hep-lat/0510111].
- [23] Y. Kuramashi *et al.* (CP-PACS Collaboration), *Proc. Sci.*, LAT2005 (2006) 226.
- [24] D. B. Kaplan, *Phys. Lett. B* **288**, 342 (1992).
- [25] Y. Shamir, *Nucl. Phys.* **B406**, 90 (1993).
- [26] V. Furman and Y. Shamir, *Nucl. Phys.* **B439**, 54 (1995).
- [27] T. Blum and A. Soni, *Phys. Rev. D* **56**, 174 (1997).
- [28] T. Blum and A. Soni, *Phys. Rev. Lett.* **79**, 3595 (1997).
- [29] T. Blum *et al.*, *Phys. Rev. D* **69**, 074502 (2004).
- [30] A. Ali Khan *et al.* (CP-PACS Collaboration), *Phys. Rev. D* **63**, 114504 (2001).
- [31] Y. Aoki *et al.*, *Phys. Rev. D* **69**, 074504 (2004).
- [32] M. A. Nowak, M. Rho, and I. Zahed, *Phys. Rev. D* **48**, 4370 (1993).
- [33] W. A. Bardeen and C. T. Hill, *Phys. Rev. D* **49**, 409 (1994).
- [34] W. A. Bardeen, E. J. Eichten, and C. T. Hill, *Phys. Rev. D* **68**, 054024 (2003).
- [35] M. A. Nowak, M. Rho, and I. Zahed, *Acta Phys. Pol. B* **35**, 2377 (2004).
- [36] A. A. Petrov, *Nucl. Phys. B, Proc. Suppl.* **142**, 333 (2005).
- [37] C. W. Bernard, T. Draper, G. Hockney, and A. Soni, *Phys. Rev. D* **38**, 3540 (1988).
- [38] R. Gupta, T. Bhattacharya, and S. R. Sharpe, *Phys. Rev. D* **55**, 4036 (1997).
- [39] N. H. Christ and G. Liu, *Nucl. Phys. B, Proc. Suppl.* **129**, 272 (2004).
- [40] G. Liu, Ph.D. thesis, Columbia University, 2003.
- [41] N. Yamada (RBC Collaboration), *Nucl. Phys. B, Proc. Suppl.* **129**, 376 (2004).
- [42] S. Ohta, H. Lin, and N. Yamada (RBC Collaboration), *Proc. Sci.*, LAT2005 (2006) 096 [hep-lat/0510071].
- [43] H.-W. Lin, S. Ohta, and N. Yamada (RBC Collaboration), *Nucl. Phys. B, Proc. Suppl.* **153**, 199 (2006).
- [44] Y. Aoki *et al.*, *Phys. Rev. D* **73**, 094507 (2006).
- [45] T. Takaishi, *Phys. Rev. D* **54**, 1050 (1996).
- [46] P. de Forcrand *et al.* (QCD-TARO Collaboration), *Nucl. Phys.* **B577**, 263 (2000).
- [47] D. Becirevic, S. Fajfer, and S. Prelovsek, *Phys. Lett. B* **599**, 55 (2004).
- [48] P. Boyle (UKQCD Collaboration), *Nucl. Phys. B, Proc. Suppl.* **63**, 314 (1998).
- [49] J. Hein *et al.*, *Phys. Rev. D* **62**, 074503 (2000).
- [50] M. di Pierro *et al.*, *Nucl. Phys. B, Proc. Suppl.* **129**, 328 (2004).
- [51] G. S. Bali, *Phys. Rev. D* **68**, 071501 (2003).
- [52] A. Dougall, R. D. Kenway, C. M. Maynard, and C. McNeile (UKQCD Collaboration), *Phys. Lett. B* **569**, 41 (2003).
- [53] A. M. Green, J. Koponen, C. McNeile, C. Michael, and G. Thompson (UKQCD Collaboration), *Phys. Rev. D* **69**, 094505 (2004).
- [54] K. C. Bowler *et al.* (UKQCD Collaboration), *Nucl. Phys.* **B619**, 507 (2001).
- [55] N. Yamada, S. Aoki, and Y. Kuramashi, *Nucl. Phys.* **B713**, 407 (2005).
- [56] S. Choe *et al.* (QCD-TARO Collaboration), *J. High Energy Phys.* **08** (2003) 022.
- [57] S. Gottlieb *et al.*, *Proc. Sci.*, LAT2005 (2006) 203 [hep-lat/0510072].
- [58] N. Brambilla *et al.*, hep-ph/0412158.
- [59] G. S. Bali, hep-lat/0608004.
- [60] J. L. Rosner *et al.* (CLEO Collaboration), *Phys. Rev. Lett.* **95**, 102003 (2005).
- [61] P. Rubin *et al.* (CLEO Collaboration), *Phys. Rev. D* **72**, 092004 (2005).
- [62] M. Andreotti *et al.*, *Phys. Rev. D* **72**, 032001 (2005).
- [63] F. Fang, *Phys. Rev. D* **74**, 012007 (2006).
- [64] M. Di Pierro *et al.*, *Nucl. Phys. B, Proc. Suppl.* **119**, 586 (2003).
- [65] S. Eidelman *et al.* (Particle Data Group), *Phys. Lett. B* **592**, 1 (2004).
- [66] G. Martinelli, C. Pittori, C. T. Sachrajda, M. Testa, and A. Vladikas, *Nucl. Phys.* **B445**, 81 (1995).
- [67] C. Dawson *et al.*, *Nucl. Phys.* **B514**, 313 (1998).
- [68] T. Blum *et al.*, *Phys. Rev. D* **66**, 014504 (2002).
- [69] K. G. Chetyrkin and A. Retey, *Nucl. Phys.* **B583**, 3 (2000).
- [70] S. Aoki, T. Izubuchi, Y. Kuramashi, and Y. Taniguchi, *Phys. Rev. D* **67**, 094502 (2003).
- [71] K. G. Chetyrkin, *Phys. Lett. B* **404**, 161 (1997).
- [72] K. G. Chetyrkin, J. H. Kuhn, and M. Steinhauser, *Comput.*

- Phys. Commun. **133**, 43 (2000).
- [73] S. Capitani, M. Luscher, R. Sommer, and H. Wittig (ALPHA Collaboration), Nucl. Phys. **B544**, 669 (1999).
- [74] J.A.M. Vermaseren, S.A. Larin, and T. van Ritbergen, Phys. Lett. B **405**, 327 (1997).
- [75] A.S. Kronfeld, Nucl. Phys. B, Proc. Suppl. **63**, 311 (1998).
- [76] K. Hornbostel (NRQCD Collaboration), Nucl. Phys. B, Proc. Suppl. **73**, 339 (1999).
- [77] D. Becirevic, V. Lubicz, and G. Martinelli, Phys. Lett. B **524**, 115 (2002).
- [78] K.J. Juge, Nucl. Phys. B, Proc. Suppl. **106**, 847 (2002).
- [79] J. Rolf and S. Sint (ALPHA Collaboration), J. High Energy Phys. 12 (2002) 007.
- [80] M. Nobes and H. Trotter, Proc. Sci., LAT2005 (2006) 209 [hep-lat/0509128].
- [81] A. Dougall, C.M. Maynard, and C. McNeile, J. High Energy Phys. 01 (2006) 171.
- [82] M.J. Booth, Phys. Rev. D **51**, 2338 (1995).
- [83] S.R. Sharpe and Y. Zhang, Phys. Rev. D **53**, 5125 (1996).
- [84] C. McNeile and C. Michael (UKQCD Collaboration), J. High Energy Phys. 01 (2005) 011.
- [85] M. Artuso *et al.* (CLEO Collaboration), Phys. Rev. Lett. **95**, 251801 (2005).
- [86] C. Aubin *et al.*, Phys. Rev. Lett. **95**, 122002 (2005).
- [87] G. Burdman and I. Shipsey, Annu. Rev. Nucl. Part. Sci. **53**, 431 (2003).
- [88] I.W. Stewart, Nucl. Phys. **B529**, 62 (1998).
- [89] M. Ciuchini, E. Franco, G. Martinelli, L. Reina, and L. Silvestrini, Z. Phys. C **68**, 239 (1995).
- [90] M. Ciuchini *et al.*, Nucl. Phys. **B523**, 501 (1998).
- [91] C.W. Bernard, T. Blum, and A. Soni, Phys. Rev. D **58**, 014501 (1998).
- [92] N. Yamada, Nucl. Phys. B, Proc. Suppl. **119**, 93 (2003).
- [93] S. Hashimoto *et al.*, Phys. Rev. D **60**, 094503 (1999).
- [94] J. Heitger, M. Kurth, and R. Sommer (ALPHA Collaboration), Nucl. Phys. **B669**, 173 (2003).
- [95] V. Gadiyak and O. Loktik, Phys. Rev. D **72**, 114504 (2005).
- [96] A. Gray *et al.* (HPQCD Collaboration), Phys. Rev. Lett. **95**, 212001 (2005).
- [97] J.C. Christensen, T. Draper, and C. McNeile, Phys. Rev. D **56**, 6993 (1997).
- [98] D. Becirevic *et al.*, Proc. Sci., LAT2005 (2006) 218 [hep-lat/0509165].
- [99] S. Aoki *et al.* (JLQCD Collaboration), Phys. Rev. D **67**, 014506 (2003).
- [100] S. Aoki *et al.* (JLQCD Collaboration), Phys. Rev. Lett. **91**, 212001 (2003).
- [101] M. Okamoto, Proc. Sci., LAT2005 (2006) 013 [hep-lat/0510113].
- [102] S. Hashimoto, Int. J. Mod. Phys. A **20**, 5133 (2005).